

## Article

# Investigating the Microwave-Assisted Extraction Conditions and Antioxidative and Anti-Inflammatory Capacities of *Symphytum officinale* WL Leaves

Kuo-Hao Lou <sup>1</sup>, Ming-Shiun Tsai <sup>2</sup>  and Jane-Yii Wu <sup>2,\*</sup> 

<sup>1</sup> Ph.D. Program of Biotechnology and Bioindustry, College of Biotechnology and Bioresources, Da-Yeh University, No. 168, University Rd., Dacun, Changhua 515006, Taiwan; kevin.khlou@gmail.com

<sup>2</sup> Department of Medicinal Botanicals and Foods on Health Applications, Da-Yeh University, No. 168, University Rd., Dacun, Changhua 515006, Taiwan; tsaims1@mail.dyu.edu.tw

\* Correspondence: jywu@mail.dyu.edu.tw; Tel.: +886-4-851-1888-2285; Fax: +886-4-8511323

**Abstract:** *Symphytum officinale* (comfrey) is a perennial herb native to West Asia and Europe. Its root extracts are commonly used as a natural remedy to treat muscle, joint, skin, and bone disorders, especially in Europe. However, more information is needed on the biomedical functions of comfrey leaves. This study's sequencing results of internal transcribed spacer and *trnL-trnF* genes showed that plants purchased from the local market were comfrey and named *S. officinale* WL (WL). The suitable extraction conditions of the WL leaves with the highest extract yield and total phenols and flavonoid contents by microwave-assisted extraction were identified. The antioxidative and anti-inflammatory activities and possible molecular mechanism(s) of the WL leaf extract (WLE) were evaluated. Furthermore, the major component of WLE was identified as rosmarinic acid by HPLC. Results showed that the optimal extract condition was obtained with 750 W microwave power, 50 °C, 75% methanol, the solid-to-solvent ratio of 1:10, and 15 min. Results of all DPPH, ABTS, and superoxide radical scavenging activities, reducing power, ferrous ion chelating activity, and ferric reducing antioxidant power showed high antioxidative capacities of WLE. Furthermore, WLE showed prominent DNA-protecting activity. WLE attenuated lipopolysaccharide-stimulated inflammation by suppressing iNOS, COX-2, IL-1 $\beta$ , IL-6, and TNF- $\alpha$  expressions in the RAW264.7 macrophages. These attenuations are involved in the inactivation of lipopolysaccharide-stimulated NF- $\kappa$ B and MAPK signaling pathways. Therefore, the comfrey leaf extract obtained via a time- and energy-saving microwave-assisted extraction may be a potential antioxidative and anti-inflammatory biomedical agent.

**Keywords:** comfrey leaf extract; microwave-assisted extraction; rosmarinic acid; antioxidant; anti-inflammation; NF- $\kappa$ B signaling; MAPK signaling



**Citation:** Lou, K.-H.; Tsai, M.-S.; Wu, J.-Y. Investigating the Microwave-Assisted Extraction Conditions and Antioxidative and Anti-Inflammatory Capacities of *Symphytum officinale* WL Leaves. *Processes* **2023**, *11*, 2750. <https://doi.org/10.3390/pr11092750>

Academic Editor: Carla Silva

Received: 19 August 2023

Revised: 7 September 2023

Accepted: 12 September 2023

Published: 14 September 2023



**Copyright:** © 2023 by the authors. Licensee MDPI, Basel, Switzerland. This article is an open access article distributed under the terms and conditions of the Creative Commons Attribution (CC BY) license (<https://creativecommons.org/licenses/by/4.0/>).

## 1. Introduction

Comfrey is a perennial herb which belongs to the borage family (Boraginaceae) and the genus *Symphytum*. It originated in Western Asia and Europe, where it liked wet places near rivers and fields. It spreads worldwide, and people grow it in gardens as a natural medicine [1]. *Symphytum* includes about 40 species, and 5 of them, including *S. officinale*, *S. asperum*, *S. peregrinum*, *S. tuberosum*, and *S. caucasicum*, are commonly used as comfrey [2]. Although *S. asperum* and *S. peregrinum* are used as comfrey, the most popular is *S. officinale* for its well-known anti-inflammatory properties [1,3].

For the past 2000 years, the roots of comfrey have enjoyed a high reputation in traditional medicine as a natural medicine, especially in Europe [4]. Root extracts have been widely used to treat muscle and joint diseases, wounds, bone fractures, and inflammation [5,6]. They are also used as topical preparations to treat ulcers, sprains, and fractures [7]. Comfrey root extract exhibits remarkable antioxidant activity [6,8], which could

be attributed to the diverse polyphenols, such as rosmarinic acid (RA), a potent antioxidant *in vitro* [9,10]. Furthermore, other phytoconstituents of comfrey, such as allantoin (which stimulates cell proliferation and improves regeneration of damaged tissues), shikonin (which suppresses the transcriptional activation of the TNF-promoter), hydrocaffeic acid (which inhibits the release of IL-1 $\beta$ ), chlorogenic acid (which inhibits productions of NO and pro-inflammatory cytokines), and rutin (which suppresses the production of TNF- $\alpha$  and IL-6, and the activation of NF- $\kappa$ B) have been identified [3]. Previous studies have shown that RA and its derivatives possess anti-inflammatory, antioxidant, antibacterial, hypoglycemic, and anti-allergic activities [2,3,11]. The European Scientific Cooperative on Phytotherapy recommends comfrey for certain conditions, such as tendinitis, knee injury, knee osteoarthritis, insect bites, mastitis, fractures, and skin inflammation [12].

Comfrey root as a medicinal product has been widely accepted and marketed in about 20 countries. However, the hepatotoxic pyrrolizidine alkaloids in comfrey limit its long-term and oral consumption [13,14]. Therefore, there is a need to improve comfrey extracts for maximizing polyphenol content while minimizing pyrrolizidine alkaloid content to produce the optimal therapeutic effects [11]. Traditional extraction methods using common petrochemical solvents have proven effective in recovering valuable compounds from plant materials. However, these conventional extraction processes have numerous drawbacks, including extended exposure times, generation of hazardous volatile organic compounds, low extraction yields, introduction of thermal effects, need for separate evaporation facilities, retention of residues after evaporation, and adverse health, safety, and environmental impacts [8,10]. In contrast, new techniques, such as ultrasound-assisted extraction (UAE) and microwave-assisted extraction (MAE), have gained wide acceptance. These methods are highly adaptable for industrial use, easy to operate, cost-effective, and demonstrate superior extraction efficiency [15–17]. In addition, they have a reduced negative environmental impact compared to conventional methods. Extractions with different solvents and filtrations with different filters can lower the alkaloid content in comfrey extracts [8,15]. Recently, comfrey leaves were extracted by the UAE method combined with a betaine–urea solvent, showing the highest RA level (1.934 mg/g). In contrast, it managed to maintain the lowest level (0.018 mg/g) of lycopsamine, one of the major pyrrolizidine alkaloids in comfrey [15].

MAE has many advantages, including faster extraction times and higher yields. However, MAE has limitations. Challenges due to sample heterogeneity, potential thermal degradation of sensitive compounds, solvent compatibility issues, and complexity of sample matrices can hinder its effectiveness [16,17]. In addition, upscaling of MAE can be difficult, and acquiring specialized equipment can be costly. Researchers and practitioners should carefully tailor MAE parameters to their specific samples to mitigate these limitations. They may consider combining MAE with complementary techniques and implementing stringent controls to ensure reliable and reproducible results. The critical parameters of MAE, such as solvent, time of extraction, ratio of solid to solvent, temperature of extraction, and power applied, can enhance the active ingredients and secondary metabolites obtained by extraction and can be adapted to different functionalities [16,17].

According to Karavaev et al. [18], comfrey leaves contain high amounts of polyphenols that can inhibit fungal pathogens. Research has also shown that comfrey leaves can fight against a variety of bacterial pathogens [19], and their polyphenols may be responsible for these antibacterial effects [20]. Furthermore, aqueous glycolic extract of *S. officinale* L. leaves shows wound healing and anti-inflammatory effects [3,21]. Since comfrey leaf extract has much fewer hepatotoxic alkaloids than the root extract and comfrey shoots and leaves contain the most rosmarinic acid, comfrey leaf extract may be a biomedical candidate [22,23]. A recent study showed that an ethanolic extract of comfrey leaves exhibits anti-enzymatic and anti-diabetic properties *in vitro* [24].

Leaves are easier than roots to mass-produce for industrial applications. The active ingredients and biological activities of comfrey leaf extract must be clarified. In this study, we aimed to explore the biomedical potential(s) of the comfrey leaf extract. The comfrey

plant was obtained from a local market and verified by molecular biology techniques. MAE was applied to obtain the maximum bioactive compounds in comfrey leaves. The optimal extraction parameters were determined by measuring the yields and total phenolic and flavonoid contents. Various methods assessed the antioxidant activities of comfrey leaf extract. The DNA protection effect of the leaf extract was also examined. The major components and their concentrations of the comfrey leaf extract were identified by high-performance liquid chromatography (HPLC). In addition, the anti-inflammatory effects and possible mechanism(s) of the comfrey leaf extract were investigated using an inflammation cell model of lipopolysaccharides (LPS)-induced murine RAW264.7 macrophages.

## 2. Materials and Methods

### 2.1. Materials (Plant and Chemicals)

The plant with the appearance characteristics of comfrey was purchased from a plant farm in Tanwei, Changhua, Taiwan.

Acetonitrile, agarose, aluminum chloride, ascorbic acid, 2,20-azino-bis-3-ethylbenzthiazoline-6-sulphonic acid (ABTS), bovine serum albumin (BSA), butylated hydroxytoluene (BHT), dimethyl sulfoxide (DMSO), 1,1-diphenyl-2-picrylhydrazyl (DPPH), 3-(4,5-dimethylthiazol-2-yl)-2,5-diphenyltetrazolium bromide (MTT), ethanol, ethylenediamine tetraacetic acid (EDTA), ferric chloride, ferrous sulfate, ferrozine, formic acid, Folin-Ciocalteu reagent, gallic acid, glycerol, hydrochloric acid, hydrogen peroxide, lipopolysaccharides (LPS), N-(1-naphthyl) ethylenediamine dihydrochloride, paraformaldehyde, phosphoric acid, potassium ferricyanide, potassium persulfate, polyacrylamide solution (29:1), pyrogallol, quercetin, rosmarinic acid (RA), sodium carbonate, sodium dodecyl sulfate (SDS), sodium hydroxide, sodium nitrite, sulfanilamide,  $\alpha$ -tocopherol, trichloroacetic acid (TCA), and Tween 20 were purchased from Merck Co. All chemicals and solvents used in this study were of analytical grade or HPLC grade. Primary antibodies against nuclear factor kappa-light-chain enhancer of activated B cells (NF- $\kappa$ B) p65, phosphorylated NF- $\kappa$ B p65, inducible nitric oxide synthase (iNOS), cyclooxygenase 2 (COX2), and  $\beta$ -actin, and secondary antibodies coupled HRP were obtained from Cell Signaling Technology. Primary antibodies against mitogen-activated protein kinases (MAPKs) and phosphorylated MAPKs were obtained from Signalway Antibody (Greenbelt, MD, USA).

The comfrey plant was planted in the garden of Da-Yeh University. After two weeks of plant acclimatization, we propagated multiple plants using root cuttings. We collected leaves periodically, washed harvested leaves with reverse osmosis (RO) water, and dried them in an oven at 60 °C for 2 days. We weighed the dry weight of these leaves and then stored them in a moisture-proof box until experiments were carried out. The flow chart of this study is shown in Figure 1.

### 2.2. Extraction of Comfrey Genomic DNA

The cetyl trimethyl ammonium bromide (CTAB) method was used to extract the genomic DNA from comfrey leaves [25]. We cut fresh comfrey leaf into 2 cm<sup>2</sup> sections and put them in a 1.5 mL sterile Eppendorf. Then, we added 500  $\mu$ L of CTAB lysate, used a grinding rod to homogenize the mixture, and then placed it in a water pot at 60 °C for an incubation period of 30 min. After centrifugation at 10,000  $\times$  g for 10 min, 300  $\mu$ L of supernatant was put into a new Eppendorf, and we added 300  $\mu$ L of chloroform–isoamyl alcohol (24:1) solution. After mixing, we centrifuged the tube at 10,000  $\times$  g for 10 min, and then 250  $\mu$ L of supernatant was obtained. After adding 175  $\mu$ L isopropanol, the tube was placed in a –20 °C refrigerator for 15 min to precipitate DNA. After centrifugation at 10,000  $\times$  g for 10 min to discard the supernatant, the DNA pellet was washed with 1 mL of ice-cold 70% ethanol. The genomic DNA was re-dissolved in 20  $\mu$ L sodium phosphate buffer (50 mM, pH 7.4) containing 1 mM EDTA and 5% glycerol and then stored at –20 °C until use.

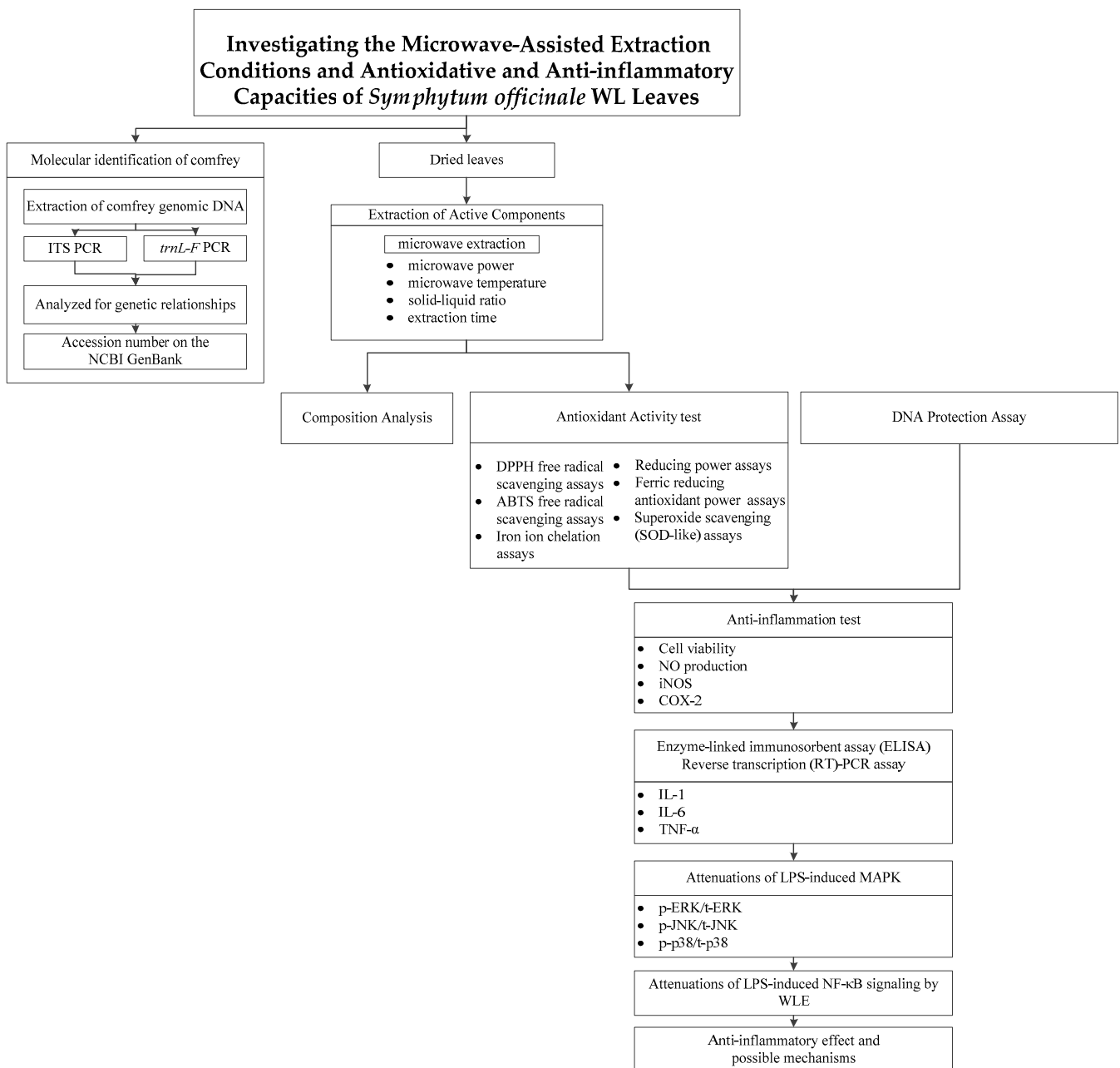


**Figure 1.** The experimental flow chart of this study.

### 2.3. Molecular Identification of Comfrey

According to the published comfrey molecular identification method, two commonly used DNA fragments, the internal transcribed spacer (ITS) of ribosomal gene and the *trnL-trnF* fragment of chloroplast, were used to conduct the taxonomic study on the genetic relationship of comfrey [26]. The names of the DNA fragments, primer names, sequences, and lengths of primers are listed in Table 1. We used ITS5-F and ITS4-R primers to amplify ITS and *trnL-trnF*-F and *trnL-trnF*-R primers to amplify *trnL-trnF* by polymerase chain reactions (PCR), respectively. PCR products were separated in a 2% agarose gel by electrophoresis, and the DNA fragments of the target lengths were excavated, purified, and entrusted to the Genomics Company (New Taipei City, Taiwan) to perform DNA sequencing. The BLAST program was used to compare the obtained DNA sequence with the sequence in the GenBank of NCBI, and then the sequences of species with high similarities were downloaded. We used the BioEdit software version 7.0.5.3

(<http://www.mbio.ncsu.edu/BioEdit/BioEdit.html>) to align all these sequences via the clustalW multiple alignment function. The phylogenetic tree analysis was drawn using the maximum likelihood method using the Tamura 3 parameter and the gamma distribution method and the neighbor-joining method using the MEGA X (Molecular Evolutionary Genetics Analysis). The internal branch strength test of the phylogenetic tree uses the analysis of 1000 replications of the bootstrap, and other parameters were preset according to MEGA X. Furthermore, the internal branch strength test of the neighbor-joining method also used the analysis of 1000 replications of the bootstrap, and the substitution model used maximum composite likelihood analysis.

**Table 1.** Gene or fragment name, primer names, sequences, and lengths of primer pairs used in this study.

Gene or Fragment Name	Primer Name	Sequence	Length (bp)
IL-1 $\beta$	IL-1 $\beta$ -mF	5'-GGGCTGCTTCCAAACCTTG	20
	IL-1 $\beta$ -mR	5'-GCTTGGGATCCACACTCTCC	20
IL-6	IL-6-mF	5'-TCCAGTTGCCTTCTTGGGAC	20
	IL-6-mR	5'-GTGTAATTAAGCCTCCGACTTG	22
TNF- $\alpha$	TNF- $\alpha$ -mF	5'-TCTCATCAGTTCTATGGCCC	20
	TNF- $\alpha$ -mR	5'-GGGAGTAGACAAGGTACAAC	20
$\beta$ -actin	$\beta$ -act-mF	5'-GTGGGCCGCCCTAGGCACCAG	21
	$\beta$ -act-mR	5'-GGAGGAAGAGGATGCGGCAGT	21
ITS	ITS5-F	GGAAGTAAAAGTCGTAACAAGG	22
	ITS4-R	TCCTCCGCTTATTGATATGC	20
trnL-trnF	trnL-trnF-F	CGAAATCGGTAGACGCTACG	20
	trnL-trnF-R	ATTGAACTGGTGACACGAG	20

mF, mouse forward primer; mR, mouse reverse primer; F, forward primer; R, reverse primer.

#### 2.4. Assays of Suitable MAE Conditions

MAE of *S. officinale* WL (WL) leaves was accomplished used the MAS-II PLUS microwave synthesis/extraction reaction apparatus (SINEO Microwave Chemistry Technology Co., Ltd., Shanghai, China). The oven-dried WL leaves were ground into fine powders (<10 mesh) using the stainless-steel grinder. The parameters of the microwave-assisted extraction conditions were discussed in order of microwave power, microwave temperature, solid-solvent ratio, and extraction time. The WL leaf powders were weighed, mixed with solvent in a 50 mL microwave extraction bottle, and then placed in the microwave instrument tank. After extraction, the solution was centrifuged at 6000 $\times$  g for 5 min to obtain supernatant and then the volume was recorded. Different extraction conditions were evaluated by yields and total phenolic and flavonoid contents.

In order to increase the extraction efficiency, shorten the extraction time, reduce the extraction temperature, and obtain more bioactive substances, we used MAE to extract bioactive substances from the dried powder of WL leaves. Therefore, several parameters of MAE were first studied individually, including microwave radiation power, extraction temperature, methanol concentration, solid-to-solvent ratio, and time of extraction. The yield (%), and total phenolic and flavonoid contents were analyzed to determine the suitable MAE conditions. This study used different concentrations of aqueous methanol as the extraction solvent. Based on the boiling point of methanol at 64 °C, the microwave power ranged from 250 W to 1000 W, the temperature ranged from 25 °C to 60 °C, the methanol concentration ranged from 0% to 100%, the solid-to-solvent ratio ranged from 1:2.5 to 1:15 (*w/v*), and the time ranged from 0.5 min to 45 min.

### 2.5. Assays of Extraction Yield

We dried 1 mL of each extraction solution in a 1.5 mL Eppendorf at 60 °C for 2 days. The dried weight of each extraction solution was recorded. The extraction yield (%) for each extraction solution was calculated using the following Equation (1):

$$\text{Yield (\%)} = (\text{Wd} \times \text{V}) / \text{Wt} \times 100\% \quad (1)$$

where Wd is the dried weight of 1 mL extraction solution, V is the volume of extraction solution, and Wt is the weight of WL leaf powder used (1 g).

### 2.6. Assays of Total Phenolic and Flavonoid Contents

Total phenolic content (TPC) of the extract was determined by the Folin–Ciocalteu assay as previously described [27]. Briefly, WL leaf extract (WLE, 1 mL) with various concentrations was mixed with 1 mL 10-fold diluted Folin–Ciocalteu reagent and 100 µL sodium carbonate (10%, w/v). After mixing, the mixture was reacted in the dark for 30 min, and then the absorbance was measured at 735 nm. TPC was expressed as gallic acid equivalents (GAE) in mg/g dry leaves.

Total flavonoid content (TFC) of the extract was determined by the aluminum chloride colorimetric method [28]. WLE (1.8 mL) with various concentrations was mixed and reacted with 0.09 mL 5% sodium nitrite solution (5%, w/v) for 6 min, followed by 0.09 mL of aluminum chloride solution (10%, w/v). Finally, after reaction for 5 min, 0.6 mL of 1 M sodium hydroxide was added to the mixture. The absorbance was measured at 510 nm. Quercetin was used as the standard compound, and the total flavonoid content was calculated using the calibration curve for quercetin. TFC are expressed as quercetin equivalents (GE) in mg/g dried leaves.

### 2.7. DPPH Free Radical Scavenging Assay

Radical scavenging activity of the WLE was determined by DPPH assay [29], with modifications. Briefly, various concentrations of WLE (1.5 mL) were added to 3 mL DPPH solution (0.2 mg/mL), and absorbance was measured at 517 nm after 30 min. Seventy-five percent of methanol was used as a blank. The BHT was used as a positive control. Radical scavenging activity was expressed as the inhibition ratio (%) using the following Equation (2):

$$\text{The inhibition ratio (\%)} = (1 - \text{Ae}/\text{Ac}) \times 100\% \quad (2)$$

where Ae is the absorbance of the WLE or positive control, and Ac is the absorbance of the blank.

### 2.8. ABTS Free Radical Scavenging Assay

An ABTS free radical scavenging assay was used [30] with modifications. Briefly, we used 7.35 mM potassium persulfate to mix 7 µM ABTS and kept it in the dark for 24 h at room temperature to promote ABTS's oxidation and generate blue-green ABTS+ free radicals. The ABTS+ solution was diluted with 95% ethanol to an absorbance value of  $1 \pm 0.05$  at 735 nm. Various concentrations of the WLE (3 mL) were added to 3 mL ABTS+ solution, and then the absorbance was measured at 750 nm. Seventy-five percent methanol was used as a blank. Ascorbic acid was used as a positive control.

### 2.9. Iron Ion Chelation Assay

An iron ion chelation assay [31] was used with modifications. Briefly, 2 mM ferrous sulfate (0.24 mL) was mixed with various concentrations of the WLE (2.4 mL). After adding 5 mM ferrozine (0.48 mL), the mixture was reacted for 10 min, and then the absorbance at 562 nm was measured. Seventy-five percent methanol was used as a blank. The positive

control used EDTA. The iron-chelating effect for ferrozine-Fe<sup>2+</sup> complex formation was calculated by the following Formula (3):

$$\text{Iron chelating effect (\%)} = [1 - (A/B)] \times 100\% \quad (3)$$

where A is the absorbance of the WLE, and B is the absorbance of a blank.

#### 2.10. Reducing Power Assay

To determine the reducing power of the WLE, the reduction of Fe<sup>3+</sup> to Fe<sup>2+</sup> was monitored as previously described [32], with some modifications. Here, 2 mL of various concentrations of the WLE, 2 mL of phosphate buffer (200 mM, pH 6.6), and 2 mL potassium ferricyanide (1%, w/v) were mixed. The mixture was incubated at 50 °C for 20 min, and then 2 mL of TCA (10%, w/v) was added. After centrifugation at 8000 × g for 3 min, 2 mL supernatant was mixed with 2 mL RO water and 0.4 mL ferric chloride (0.1%, w/v). After 10 min of reaction, the absorbance at 700 nm was measured against a blank. Ascorbic acid was used as a positive control.

#### 2.11. Ferric Reducing Antioxidant Power (FRAP) Assay

The FRAP assay was used [33] with some modifications. The WLEs (0.6 mL) with various concentrations were mixed with 2.4 mL FRAP reagent and then incubated in the dark at 37 °C for 10 min. The absorbance at 593 nm was measured. Ascorbic acid was used as a positive control. The results were expressed as ascorbic acid equivalent in mM ascorbic acid.

#### 2.12. Superoxide Scavenging (SOD-Like) Assay

SOD-like assay was used as reported [34]. Briefly, various concentrations of the WLE (1 mL) were mixed with 1 mL Tris-HCl buffer (pH 7.4) and 0.5 mL pyrogallol solution (in 1 M hydrochloric acid). After mixing and incubation for 5 min at 37 °C, the absorbance was measured at 325 nm. The ΔA (325 nm, control) value reflected the initial concentration of substrate •O<sub>2</sub><sup>-</sup>, so this value should be well controlled to guarantee the accuracy of method. Seventy-five percent methanol was used as a control. The following Formula (4) was used to calculate the percentage of superoxide radical scavenging activity:

$$\text{Activity (\%)} = [(\Delta A_{325, \text{control}})/T - (\Delta A_{325, \text{sample}})/T]/[(\Delta A_{325, \text{control}})/T] \times 100\% \quad (4)$$

where ΔA<sub>325, control</sub> is the ΔA<sub>325</sub> of control; ΔA<sub>325, sample</sub> is the ΔA<sub>325</sub> of various concentrations of WLE; T is the reaction time (5 min).

#### 2.13. DNA Protection Assay

DNA damage could be detected by the conversion of supercoiled pCIneo plasmid DNA into the nicked circular or degraded forms, as previously described [35], with slight modifications. Here, 20 μL of a reaction mixtures containing 2.5 μL of supercoiled pCIneo (150 ng/μL), 10 μL of the Fenton reagent containing 30 mM hydrogen peroxide, 100 μM ferric chloride, and 100 μM ascorbic acid in 20 mM Tris-HCl buffer (pH 7.6), and 5 μL of various concentrations of the WLE or 250 ng/mL quercetin (a nicked control), were used. After incubation at 37 °C for 30 min, the plasmid DNAs in the reaction mixture were separated on a 1% agarose gel and then stained with SafeView™ (Applied Biological Materials Inc. Richmond, BC, Canada). To quantify the DNA protective activity of the WLE, the amounts of supercoiled and nicked forms of pCIneo were quantified by the AlphaImager Mini instrument (BIO-TECHNE Co., Minneapolis, MN, USA), and the band intensity on agarose gel was quantified by GelPro software (Gel-Pro analyser software version 3.0). As negative and positive controls, pCIneo plasmid was incubated alone and with the Fenton reagent, respectively. The DNA protective activity of the WLE was

calculated from the quantity of supercoiled or nicked plasmid DNAs by using the following Equations (5) and (6):

$$\text{Protection of supercoiled plasmid (\%)} = \frac{\text{band intensity of supercoiled form}}{\text{band intensity of pCIneo supercoiled DNA}} \times 100\% \quad (5)$$

$$\text{Percentage of nicked plasmid (\%)} = \frac{\text{band intensity of nicked form}}{\text{band intensity of total pCIneo plasmid DNA}} \times 100\% \quad (6)$$

#### 2.14. HPLC Assays

The HPLC instruments used in this study consisted of the Hitachi HPLC D-2000 System (E HONG Instruments Co., Ltd., Taipei, Taiwan) and SPD-10A VP photodiode array detector (Shimadzu, Scientific Instruments Co., Ltd., Taipei, Taiwan). A Scpak ODS-P C18 column (5  $\mu\text{m}$ , 4.6 mm ID  $\times$  250 mm) (Analab Co., Taipei, Taiwan) was used. The mobile phase was 0.1% aqueous formic acid (A) and 0.1% formic acid in acetonitrile (B) using an elution gradient of 5–95% B at 0–44 min and 5% B at 44–49 min. WLE and various concentrations of RA (20  $\mu\text{L}$ ) were filtered through a 0.45  $\mu\text{m}$  Minipore filter (Minipore Micro Products) before injection into the column, respectively. The flow rate was 1.0 mL/min with the detection wavelength at 280 nm. RA was dissolved in 99.5% ethanol. RA in various concentrations were used to obtain a standard curve for calculating the RA concentration in the WLE.

#### 2.15. Cell Culture

Murine RAW 264.7 macrophages (BCRC 60001) were purchased from the Bioresource Collection and Research Center (Hsinchu, Taiwan) and cultured in Dulbecco's modified Eagle's medium supplemented with 10% heat-inactivated fetal bovine serum, 1% penicillin-streptomycin and 2 mM L-glutamine (Biological Industries Ltd., Kibbutz Beit-Haemek, Israel) at 37 °C in the 5% CO<sub>2</sub> humidified animal cell incubator. The WLE used in cell culture was re-dissolved and diluted in DMSO to various concentrations.

#### 2.16. Cell Viability Assay

The cell viability was determined by MTT assay as previously described [36]. RAW 264.7 macrophages were cultured at a cell density of  $5 \times 10^4$  cells/well in a 96-well plate for 24 h. Cultured cells were treated with or without 10 ng/mL LPS and various concentrations of the WLE for another 24 h. Cells were washed with phosphate-buffered saline (PBS, pH 7.4), and then MTT in Dulbecco's modified Eagle's medium was added. After incubation for 3 h, 10% DMSO was added to dissolve the formed formazan. The absorbance at 570 nm was measured.

#### 2.17. Nitrite Determination

Amounts of nitrite in the culture media were determined using Griess reagent kit (Abcam plc., Blossom Biotechnologies Inc., Taipei, Taiwan). RAW 264.7 macrophages were seeded onto 6-well plates ( $5 \times 10^5$  cells/well) and then incubated cells for 24 h. Cultured cells were treated with or without 10 ng/mL LPS and various concentrations of WLE for another 24 h. Subsequently, 100  $\mu\text{L}$  of supernatant from each well was transferred onto a 96-well plate. Each well was supplemented with 100  $\mu\text{L}$  of Griess reagent containing 0.1% N-(1-naphthyl) ethylenediamine dihydrochloride and 1% sulfanilamide in 5% phosphoric acid for 10 min. The absorbance of each solution was measured at 540 nm, and the concentrations of nitrite were calculated by a standard calibration curve established using different concentrations of sodium nitrite.

#### 2.18. Reverse Transcription (RT)-PCR Assay

RAW 264.7 macrophages were seeded onto 6-well plates ( $5 \times 10^5$  cells/well) and then incubated for 24 h. Cultured cells were treated with or without 10 ng/mL LPS and various concentrations of the WLE for another 24 h. The total RNAs were extracted using Trizol

reagent and then reversely transcribed using a Superscript III system (Life Technologies). The primer pairs used to determine the expressions of interleukin (IL)-1 $\beta$ , IL-6, tumor necrosis factor (TNF)- $\alpha$ , and  $\beta$ -actin cDNAs by PCR are shown in Table 1.

#### 2.19. Enzyme-Linked Immunosorbent Assay (ELISA)

RAW 264.7 macrophages were seeded at a density of  $1 \times 10^5$  cells/well in 6-well plates for 24 h. Cultured cells were treated with or without 10 ng/mL LPS and various concentrations of the WLE for another 24 h. After centrifugation of media, supernatants were transferred into a 96-well plate and the IL-1 $\beta$ , IL-6, and TNF- $\alpha$  concentrations were quantified using ELISA kits (China Rhenium Co., Ltd., Zhuzhou, China) according to the manufacturer's instructions. The absorbance at 450 nm was measured and the absolute concentration was calculated using the standard curve.

#### 2.20. Western Blots

RAW 264.7 macrophages at a density of  $2 \times 10^5$  cells/well were seeded in 6-well plates for 24 h. Cultured cells were treated with or without 10 ng/mL LPS and various concentrations of the WLE for another 24 h. After washing with PBS, cells were treated with RIPA buffer containing protein inhibitor cocktail (Abcam plc., Blossom Biotechnologies Inc., Taipei, Taiwan) for cell lysis and then centrifuged at  $12,000 \times g$  at 4 °C for 15 min to collect the cellular proteins. Cellular proteins were separated using 4–12% SDS-polyacrylamide gradient gels and then transferred onto polyvinylidene difluoride membranes (Sigma-Aldrich. Uni-onward Corp., New Taipei, Taiwan). After blocking, membranes were incubated with specific primary antibodies (1:1000 dilution) for detecting mouse NF- $\kappa$ B p65, phosphorylated NF- $\kappa$ B p65, iNOS, COX2, MAPKs, and phosphorylated MAPKs, respectively. After reactions with coupled secondary antibodies, protein signals were developed using enhanced chemiluminescence (Sage Creation, Chaoyang, Beijing, China) and then they were determined using AlphaEase FC software (version 6.0) (Alpha Innotech, Watertown, MA, USA).

#### 2.21. NF- $\kappa$ B Nuclear Translocation Assay

RAW 264.7 macrophages at a density of  $2 \times 10^4$  cells/well were planted in a 24-well plate with 12 mm chamber slides for 24 h. Cultured cells were treated with or without 10 ng/mL LPS and 500  $\mu$ g/mL of the WLE for another 24 h. Cells in 12 mm chamber slides were washed with PBST (PBS containing 1% Tween 20) and fixed with 4% paraformaldehyde for 15 min. Specimens were blocked with blocking buffer (PBST with 2.5% BSA) for 1 h at room temperature and then incubated with mouse anti-phosphorylated p65 antibody (1:100) at 4 °C overnight. Cells were washed with PBST 3 times and then incubated with goat anti-mouse fluorescein isothiocyanate antibody (1:200, Sigma-Aldrich) in the dark for 1 h. Cell nuclei were stained with 1 mg/mL 4',6-diamidino-2-phenylindole (DAPI) for 15 min. After being rinsed with PBS and covered with SlowFade antifade reagent (Thermo Fisher Scientific, Taiwan Co., Ltd., Taipei, Taiwan), the nuclear translocations of the phosphorylated p65 protein were assayed using a fluorescent microscope (OLYMPUS CKX41. Yuanyu Group Co., Ltd., Taipei, Taiwan). To detect the subcellular regions of the phosphorylated p65 protein, images of the same field were merged with OLYMPUS cellSens software (Olympus cellSens Entry 1.11 software).

#### 2.22. Statistical Analyses

All data are expressed as means  $\pm$  standard deviation (SD) from at least three independent experiments. Differences between treatments were identified using ANOVA followed by Dunnett's test or the Student's *t*-test. Difference was considered to be significant when  $p < 0.05$ .

### 3. Results and Discussion

#### 3.1. Molecular Identification of Native Comfrey Species

In order to determine the correct scientific name of the purchased plant, we used molecular biological identification and classification for this plant species. The CTAB DNA extraction method was used to exclude the metabolic interference of plants. The concentration of plant chromosomal DNA obtained was 8.04  $\mu\text{g}/\mu\text{L}$ , the absorbance ratio of 260/280 was 2.242, and the absorbance ratio of 260/230 was 1.952. The efficiency and quality of extracted plant chromosomal DNA were consistent with those described previously [25].

The genetic relationship of this plant was carried out using the ITS DNA fragment and the chloroplast *trnL-trnF* gene fragment by PCRs [26]. The length of the ITS fragment of this plant was in the range of 700–800 bp, while the length of the *trnL-trnF* fragment was in the range of 900–1000 bp. The lengths of the ITS and *trnL-trnF* fragments matched the *Symphytum* species.

After DNA sequencing, the DNA sequences of ITS and *trnL-trnF* fragments were analyzed for genetic relationships using the maximum parsimony method of MEGA X software (MEGA 11.0.10) and tree structure analysis. The results in Figure 2A showed that the ITS sequences showed a good partitioning among the species of *Symphytum*, and the plant used in this study was identical (100% similarity) to the ITS sequence of *S. officinale* with the accession number of MH645788.1 on the NCBI GenBank. The *trnL-trnF* fragment of this plant reached 88% similarity with the *S. officinale* sequence of accession number JQ041857.1 in the NCBI GenBank (Figure 2B). From the obtained DNA sequence similarities, we named the plant used in this study as *S. officinale* WL, abbreviated as WL.

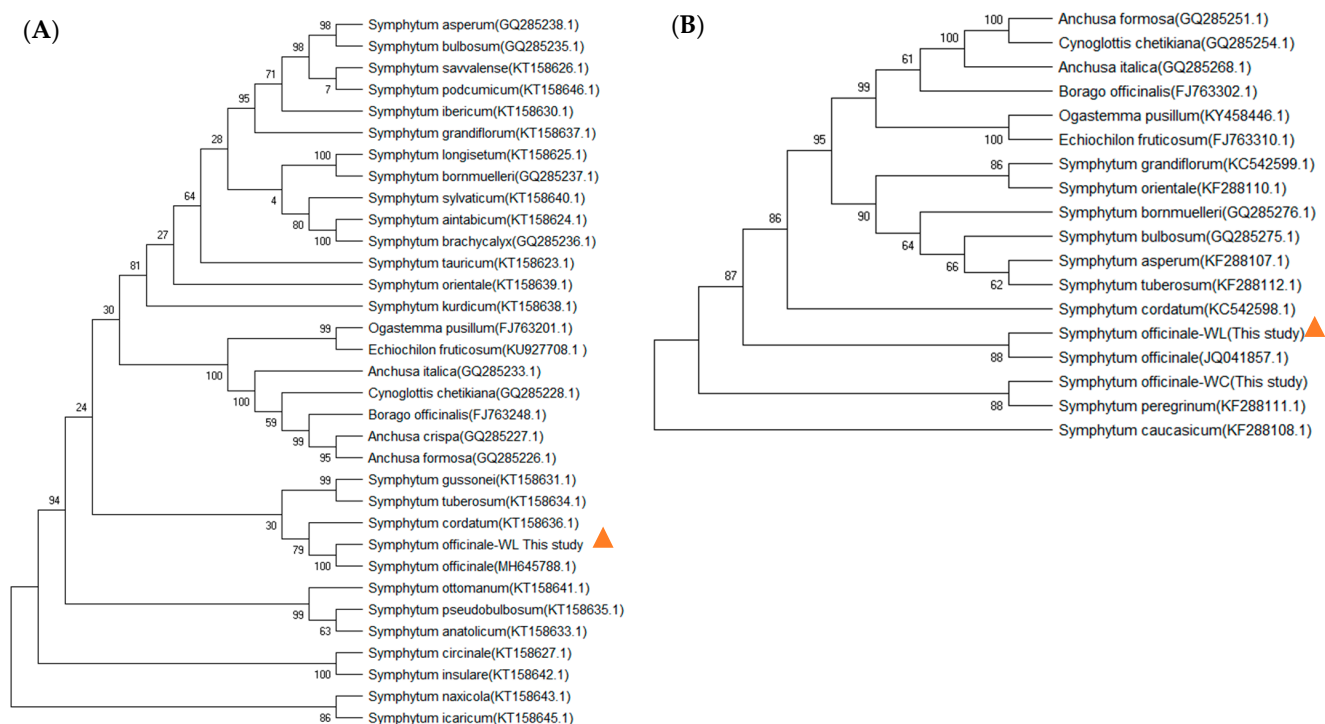


**Figure 2.** Results of sequence analyses of ITS (A) and *trnL-trnF* (B) by maximum parsimony. The orange triangles indicate the positions of the *S. officinale* WL.

#### 3.2. The Suitable MAE Conditions of WLE

##### 3.2.1. The Microwave Radiation Power

The effects of microwave powers of 250, 350, 500, 750, and 1000 W on the yields were investigated at an extraction temperature of 50 °C, a solid-to-solvent ratio of 1:10, a solvent of 75% methanol, and an extraction time of 30 min. The results showed that

the order of the yields was 250 W (10.93%) < 1000 W (11.50%) < 350 W (11.75%) < 500 W (11.18%) < 750 W (12.50%). Except for 1000 W, the yield tended to increase with increasing microwave power. Furthermore, the total phenolic and flavonoid contents decreased with increasing microwave power, except for the highest content at 750 W. It can be concluded that although increasing the microwave radiation power can promote the release of leaf substances into the solvent, too high a power may damage the active ingredients in leaves. These preliminary results showed that 750 W was the most suitable microwave power for extracting WL leaves.

### 3.2.2. The Microwave Temperature

The effects of 25, 30, 40, 50, and 60 °C microwave temperatures on the yields were investigated under a microwave power of 750 W, extraction time of 30 min, solid-to-solvent ratio of 1:10, and solvent of 75% methanol. The results showed that the order of the yields was 30 °C (11.67%) < 25 °C (11.70%) < 40 °C (12.74%) < 60 °C (12.89%) < 50 °C (13.72%). The yield increased with increasing temperature, except for at 60 °C. The results of total phenolic and flavonoid contents were consistent with the trend of extraction yields. This result indicated that the extracted phenols and flavonoids from WL leaves at temperatures below 50 °C are relatively stable. However, when the temperature exceeded 50 °C, the decomposition of the main components decreased the yield and the total phenolic and flavonoid contents. Therefore, 50 °C was identified as the most suitable extraction temperature, which was similar to the results of previous studies on extractions of the litchi fruit pericarp [37] and the pistachio green hull [38].

### 3.2.3. The Aqueous Methanol Concentration

The effects of 0%, 25%, 50%, 75%, and 100% methanol on the yields were investigated at a microwave power of 750 W, an extraction temperature of 50 °C, a solid-to-solvent ratio of 1:10, and an extraction time of 30 min. Results showed that 50% methanol was the most effective concentration for the yields, but all of these yields were 14–15% without any significant difference. However, 75% methanol could extract the greatest amounts of total phenols and total flavonoids. Previous studies have shown that 50% to 80% methanol has been used to extract hydroxycinnamic acids and many flavonoid molecules from plants [39]. It has also been suggested that the extraction of anthocyanins from plants with 70% methanol has a higher extraction rate than water extraction [40]. Diluted methanol was found to be the optimal solvent for extracting total phenols and para-hydroxycinnamic acids from green tea than diluted acetone or ethanol [41]. Therefore, we chose 75% methanol as the most suitable extraction solvent.

### 3.2.4. The Solid-to-Solvent Ratio

Effects of different solid-to-solvent ratios on the yields were investigated at a microwave power of 750 W, an extraction temperature of 50 °C, a solvent of 75% methanol, and an extraction time of 30 min. Results showed that the order of the yields was 1:2.5 (9.27%) < 1:15 (10.875%) < 1:10 (13.58) < 1:7.5 (15.18%) < 1:5 (16.00%). The highest yield was obtained when the solid–solvent ratio was increased to 1:5. The total phenol and flavonoid contents were increased with the increased solid-to-solvent ratio. However, it decreased the concentrations of total phenols and flavonoids in solution. This result is consistent with previous extraction studies [32,37]. Although the highest total phenolic content was found at a solid–solvent ratio of 1:15, the highest total flavonoid content was found at a solid–solvent ratio of 1:10. To decrease the solvent volume, a solid–solvent ratio of 1:10 was chosen.

### 3.2.5. The Extraction Time

Effects of different extraction times on the yields were investigated under a microwave power of 750 W, extraction temperature of 50 °C, solvent of 75% methanol, and a solid–solvent ratio of 1:10. Results showed that the longer the extraction time,

the higher the yield. However, the total flavonoids and phenols reached the plateau of 64.22 mg/g and 13.13 mg/g after 10 min of extraction time, respectively. The longer extraction time may cause unexpected reaction(s), such as enzyme degradation and oxidation, that may destroy polyphenols [42]. Therefore, reducing the extraction time can reduce the energy and cost and the damage and oxidation of chemicals in the plant. Based on these considerations, the suitable time for MAE was 15 min.

In summary, the suitable condition for MAE of the WL leaves was a microwave power of 750 W, extraction temperature of 50 °C, solvent of 75% methanol, solid-to-solvent ratio of 1:10, and extraction duration of 15 min. Results of the yields and the contents of total phenols and total flavonoids of each extraction condition are shown in Table 2.

**Table 2.** Results of the yields and contents of total polyphenols and flavonoids of WL leaves obtained with the optimal MAE conditions.

Extraction Condition	Suitable Condition	Yield (%)	Total Phenols <sup>1</sup> (mg/g)	Total Flavonoids <sup>2</sup> (mg/g)
Microwave power (W)	750	12.50 ± 0.42	7.39 ± 0.21	44.70 ± 1.38
Temperature (°C)	50	13.72 ± 0.65	9.12 ± 0.01	60.08 ± 0.50
Methanol concentration (%)	75	14.43 ± 0.09	8.44 ± 0.08	66.98 ± 0.80
Solid-to-solvent ratio ( <i>w/v</i> )	1:10	13.58 ± 0.01	9.09 ± 0.12	55.38 ± 0.72
Time (min)	15	16.38 ± 0.57	13.14 ± 0.17	64.23 ± 0.00

<sup>1</sup> Total phenolic content was expressed as GAE in mg/g of dried leaves. <sup>2</sup> Total flavonoid content was expressed as GE in mg/g of dried leaves.

### 3.3. Antioxidant Capacity of WLE

In order to obtain a large amount of WLE for various bioactivity analyses, we used MAE to extract the WLE under the previously discussed suitable conditions (Table 2). After extraction, the WLE was concentrated under reduced pressure and then freeze-dried. The WLE was re-solubilized in 75% methanol and diluted to 31.25, 62.5, 125, 250, 500, 1000, 2000, and 4000 µg/mL in concentrations. The WLE was evaluated for various antioxidant capacities.

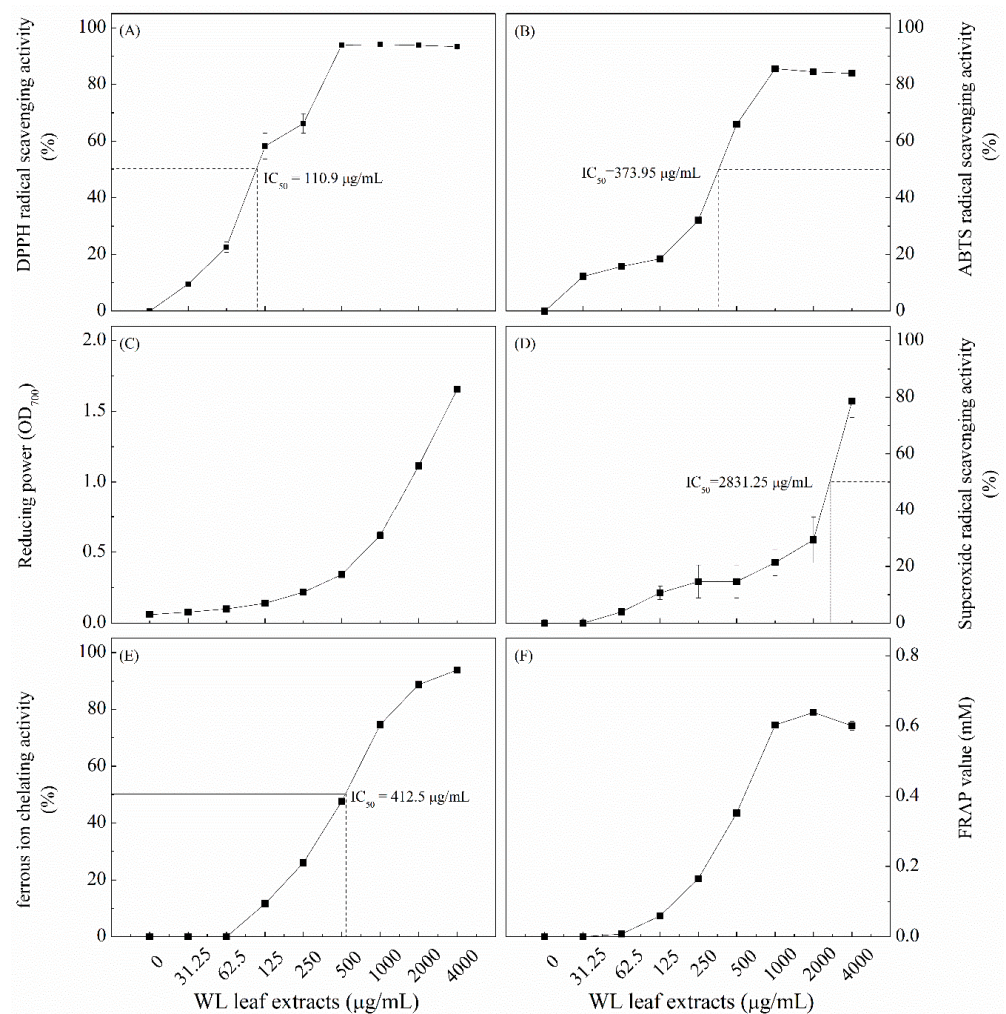
The DPPH radical scavenging activity assay was analyzed first. Figure 3A showed that the DPPH radical scavenging activity of the WLE reached the plateau and was similar to the effect of 4000 µg/mL BHT (87.2%) when concentrations of WLE ≥ 500 µg/mL. The calculated IC<sub>50</sub> value of the WLE in the DPPH radical scavenging activity was 110.9 µg/mL.

Figure 3B showed the highest ABTS radical scavenging activity at the concentration of WLE ≥ 1000 µg/mL, which was similar to the effect of 1% ascorbic acid (87.2%). The calculated IC<sub>50</sub> value of the WLE in the ABTS radical scavenging activity was 373.95 µg/mL.

Figure 3C showed that the higher the concentrations of the WLE, the higher the reducing power. At 4000 µg/mL, the reducing power of the WLE was 1.654, which was lower than the power of ascorbic acid (3.975) with the same concentration.

Figure 3D showed that the higher the concentrations of the WLE, the higher the SOD-like activity. The highest SOD-like activity was found at 4000 µg/mL (78.6%), lower than ascorbic acid (100%) at the same concentration. The IC<sub>50</sub> value of the WLE in the SOD-like activity was 2831.25 µg/mL.

The concentration of the WLE at 4000 µg/mL showed the highest ferrous ion chelating activity (93.8%), which was similar to the effect of 100 µg/mL EDTA (96.68%) (Figure 3E). The IC<sub>50</sub> value of the WLE in the ferrous ion chelating activity was 412.5 µg/mL.



**Figure 3.** Antioxidant capacities of the WLE were analyzed in terms of DPPH radical scavenging activity (A), ABTS radical scavenging activity (B), reducing power (C), superoxide radical scavenging activity (D), ferrous ion chelating activity (E), and FRAP value (F). The used concentrations of the WLE were indicated. Calculated IC<sub>50</sub> values in panels (A,B,D,E) were also indicated.

The results of Figure 3F also showed that the higher the concentrations of the WLE, the higher the ferrous reducing antioxidant power (FRAP value). The maximum FRAP value (0.638 µM) of the WLE was reached at 2000 µg/mL.

We used six commonly used methods to decipher the antioxidant capacities of WLE. There are fewer antioxidant studies on the antioxidant activity of the comfrey leaf extract than the root extract. The contained polyphenols of comfrey root extract play essential roles in scavenging free radicals [6], and high total phenolic content is associated with SOD-like capacity [43]. A previous study showed that the IC<sub>50</sub> value of DPPH radical scavenging activity of ethanol extract of comfrey leaves was 39.97 µg/mL [43], which is lower than the IC<sub>50</sub> value (110.9 µg/mL) of WLE (Figure 3A). The ABTS radical scavenging activity, reducing power, SOD-like activity, ferrous chelating activity, and FRAP value showed the same trend with DPPH radical scavenging activity, which all increased with the WLE concentration. In this study, the MAE of WL leaves was carried out, and the most suitable extraction conditions were chosen to maximize the total phenolic and flavonoid contents. The WLE obtained was rich in total phenols and flavonoids; thus, it had a relatively high antioxidant capacity.

### 3.4. DNA Protective Assay of WLE

Reactive oxygen species (ROS) are well known to damage DNA and then lead to human diseases or aging. DNA protective assay offers an in vitro model for sensitively determining the protective effects of sample from the DNA damaging radicals [44]. In this experiment, Fenton reactions produce hydroxyl radicals that cleave supercoiled DNA and convert it to the nicked form, which shows decreased electrophoretic mobility, and then can subsequently degrade the nicked DNA [45,46]. Plasmids with supercoiled and nicked forms were directly distinguished by their relative electromobilities on agarose gel electrophoresis. To evaluate the DNA protection activity of the WLE, pCIneo plasmid DNAs were reacted with the Fenton reagent and with or without the WLE. Figure 4A shows that supercoiled DNA moved faster, and that nicked DNA moved slower. When treated with the Fenton reagent (lane 2), the plasmid DNA in supercoiled form was significantly decreased to about 44% of the original plasmid (lane 1), and the nicked DNA was only about 33% of the total DNA. These results indicated that the treatment of the Fenton reagent degraded about one-third of plasmid DNA. In lane 3, almost all plasmid DNA was converted into a nicked form when Fenton reagent and quercetin were added. These results indicated that quercetin only effectively protected nicked DNA from subsequent degradation by the Fenton reagent, as previously reported [47]. In contrast, following treatments with the WLE (Figure 4A), WLE significantly reduced DNA damages at concentrations of 16.5–1000 µg/mL, protecting supercoiled forms by 25–94%, respectively (Figure 4B, lanes 4–10). The DNA protection effects of WLE had reached the plateau in the 125–1000 µg/mL concentration range. Thus, in vitro DNA protection results showed that the WLE could prevent nick and subsequent degradation of plasmid DNA and keep it in a supercoiled form. The DNA protection effect of WLE is much higher than that of leaf extracts of *Cinnamomum osmophloeum* Kanehira and *Vernonia amygdalina* [48,49]. These are the first data to show a protective effect of comfrey extract on in vitro DNA damage by Fenton reactions. Due to their previously acknowledged antioxidant capacity, DNA protections from the WLE are likely due to its phenolic and flavonoid compounds.

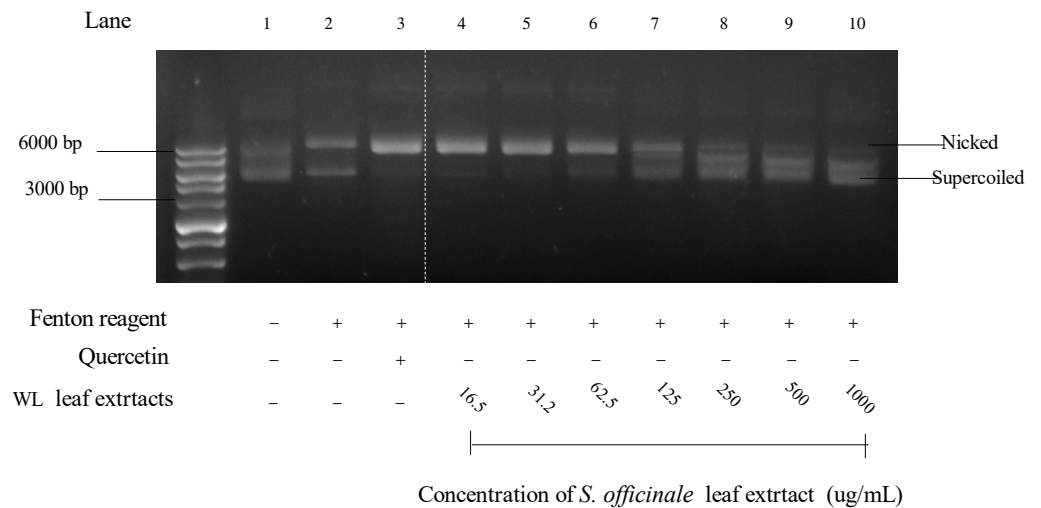
### 3.5. Composition Analysis of WLE

Root extracts are the most frequently investigated constituents for comfrey. Root extracts contain active ingredients, such as allantoin, RA, caffeic acid, and salvianolic acids [50]. However, constituents need to be explored in the leaf part. The literature suggests that RA, p-hydroxybenzoic acid, caffeic acid, and chlorogenic acid are present in the leaf, stem, and root extracts of *S. officinalis* and *S. cordatum* [23].

In order to identify the significant components in WLE, 4000 µg/mL WLE was prepared and analyzed by HPLC for its major components. The HPLC analysis was carried out under the same conditions using RA as a standard. The HPLC profile of RA is shown in Figure 5c; the HPLC profile of the WLE is shown in Figure 5b. The results showed that RA was the main component of the WLE. The quantification of RA in the WLE was calculated by the standard curve obtained from HPLC profiles with different concentrations of RA. The RA concentration in WLE was 33.0 mg/g. A previous study used ethanol to extract the comfrey roots. It analyzed the polyphenols in the extract, which showed that RA is the primary polyphenol in comfrey root extract with the highest concentration of 1.85 mg/g [6]. Comfrey root extract using 65% ethanol showed that the significant polyphenolic constituents were RA and salvianolic acid, in which RA showed the highest content of 7.557 mg/g [11]. Recently, the UAE method that coupled betaine–urea solvent to extract comfrey leaves obtained the highest 1.934 mg/g RA [15]. To compare the efficacy of MAE with UAE, we used a similar condition for UAE of WL leaves with an ultrasonic power of 600 W, temperature of 50 °C, 75% methanol as solvent, solid-to-solvent ratio of 1:15, and time of 15 min using a model DC400H ultrasonic machine (DELTA, New Taipei city, Taiwan). The WLE obtained by UAE was analyzed by HPLC using the same condition. The HPLC profile of WLE obtained by UAE is shown in Figure 5a. RA was also the primary component in this WLE obtained by UAE, although it showed lower intensity than that of

WLE by MAE. After calculation, the RA concentration of the WLE obtained by UAE was 29.5 mg/g, which was lower than the RA concentration obtained by MAE (33.0 mg/g).

(A)



(B)

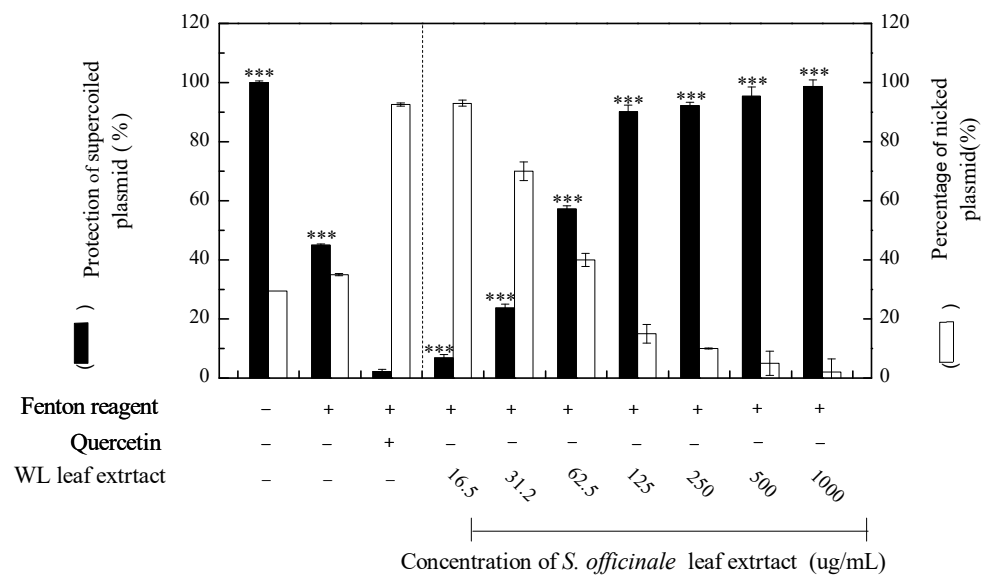


**Figure 4.** Results of DNA protective assay of WLE. (A) The photograph of DNA gel electrophoresis; (B) the quantitation results of protection of supercoiled plasmid and percentage of nicked plasmids. Treated with (+) or without (-) Fenton reagent, quercetin, and WLE were indicated. The used concentrations of WLE were indicated. \*\*\* ( $p < 0.001$ ) denotes significant difference compared with Fenton reagent and quercetin treatment group (lane 3).

In this study, we used MAE to obtain the WLE, which yielded high contents of total phenols and total flavonoids. We found that RA was the primary polyphenol in the WLE, and the RA concentration in the WLE was the highest among all published comfrey extracts.

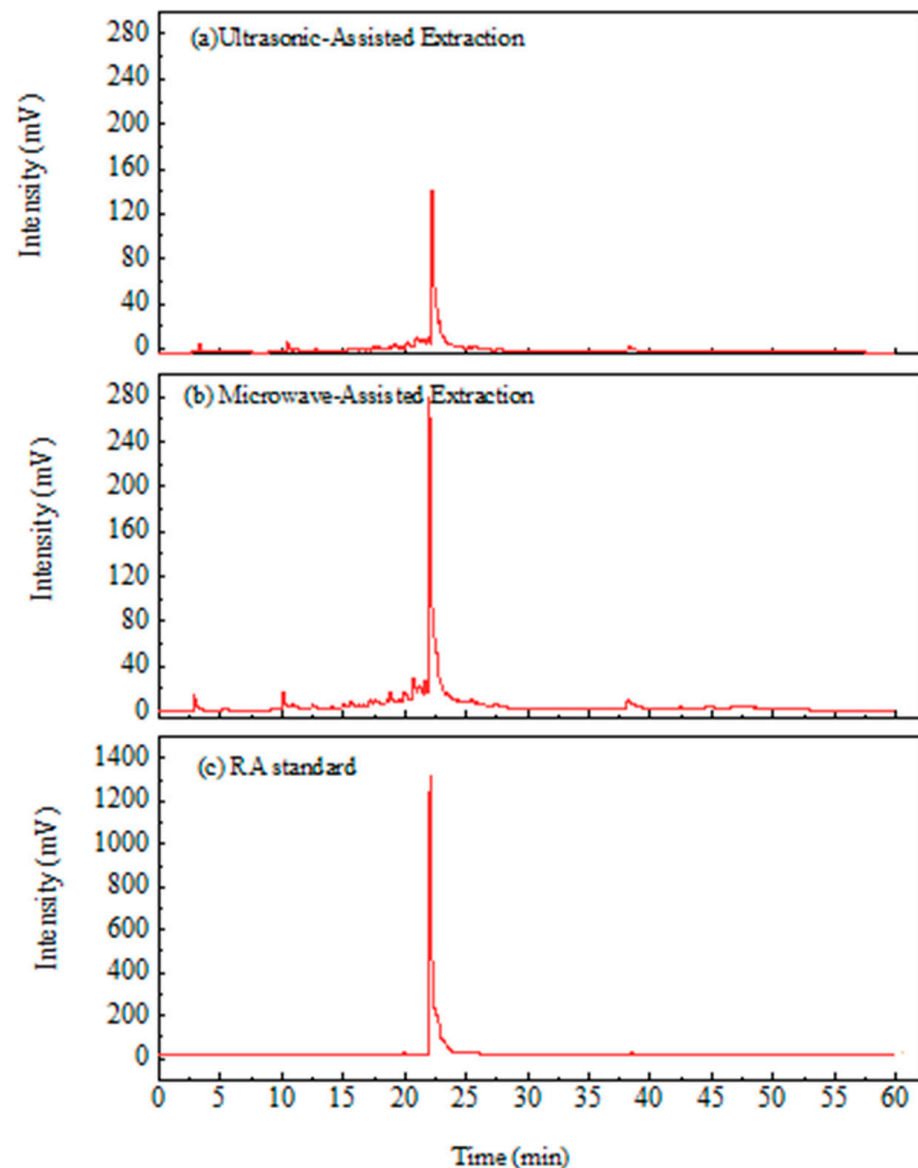


**Figure 5.** Fingerprint profiles of WLE obtained by the ultrasonic-assisted extraction (a), MAE (b), and the RA standard (c) by HPLC.

### 3.6. Anti-Inflammatory Effects of WLE

Comfrey is used in traditional medicine for its anti-inflammatory activity. Its active ingredients, such as allantoin, polyphenols, flavonoids, and alkaloids, act with multiple purposes in signaling pathways, limiting pro-inflammatory enzymes and alleviating the construction of inflammatory chemokines and cytokines, thereby inhibiting the inflammatory process [3].

To decipher the anti-inflammatory activity and possible mechanism(s) of the WLE, the standard inflammatory cell model of LPS-stimulated RAW 264.7 macrophages was used. First, we investigated the cytotoxicity of various concentrations of the WLE via MTT assay. Figure 6A shows that concentrations of WLE lower than 1000  $\mu\text{g}/\text{mL}$  had no significant effect on the viability of RAW 264.7 macrophages. To demonstrate the anti-inflammatory activity of the WLE first, we analyzed the LPS-stimulated NO (nitrite) production. Treatments with the WLE inhibited LPS-induced NO productions in a dose-dependent manner in RAW 264.7 macrophages (Figure 6B). Concentrations of the WLE higher than 125  $\mu\text{g}/\text{mL}$  showed significant inhibitory effects on LPS-induced NO production.

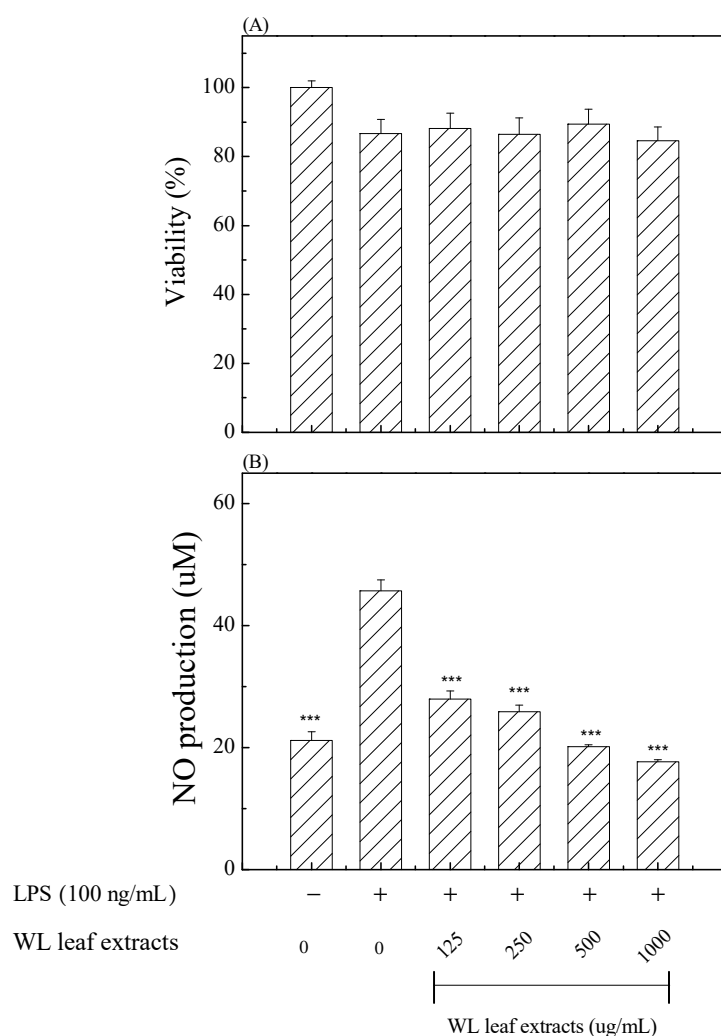


**Figure 6.** (A) Viability results of RAW264.7 macrophages treated with indicated concentrations of the WLE. (B) NO production of LPS-induced RAW264.7 macrophages treated with indicated concentrations of the WLE. Treated with (+) or without (−) LPS and WLE were indicated. The used concentrations of the WLE were indicated. \*\*\* ( $p < 0.001$ ) denotes significant difference compared with the LPS-only treated group.

Both iNOS and COX-2 are key enzymes that mediate the inflammatory process. Inappropriate upregulation of iNOS and COX-2 expression may lead to inflammatory or neoplastic diseases [51]. Next, we analyzed the effects of the WLE on LPS-stimulated iNOS and COX-2 expressions by Western blotting. The WLE showed dose-dependent inhibition of LPS-induced iNOS (Figure 7(a1,a2)) and COX-2 (Figure 7(b1,b2)) production. Combined with the results of Figures 6B and 7(a1,a2), this indicated that inhibition of NO production by the WLE might result from inhibiting iNOS expression.

IL-1 $\beta$ , IL-6, and TNF- $\alpha$  are potent pro-inflammatory factors that regulate the release of many inflammatory cytokines and the activation of immune cells [52]. To further explore the molecular mechanism(s) of the WLE in LPS-stimulated macrophages, effects of different concentrations of the WLE on LPS-induced proinflammatory cytokines, including IL-1 $\beta$ , IL-6, and TNF- $\alpha$ , were studied. To further explore the molecular mechanisms of WLE in LPS-stimulated macrophages, the effects of different concentrations of WLE on LPS-induced pro-inflammatory cytokines, including IL-1 $\beta$ , IL-6, and TNF- $\alpha$ , were investigated. The relative mRNA levels and protein expression concentrations of these pro-inflammatory cytokines were shown (Figure 8). The results showed that the WLE significantly reduced LPS-induced IL-1 $\beta$  (a1), IL-6 (b1), and TNF- $\alpha$  (c1) protein concentrations in a dose-dependent manner.

Likewise, the WLE also significantly reduced LPS-induced *IL-1 $\beta$*  (a2), *IL-6* (b2), and *TNF- $\alpha$*  (c2) gene expressions in a dose-dependent manner. The inhibitions of gene expressions and protein concentrations of these three pro-inflammatory cytokines were positively correlated. At 125  $\mu\text{g}/\text{mL}$ , WLE was the most effective at inhibiting LPS-induced IL-6 mRNA and protein expression.

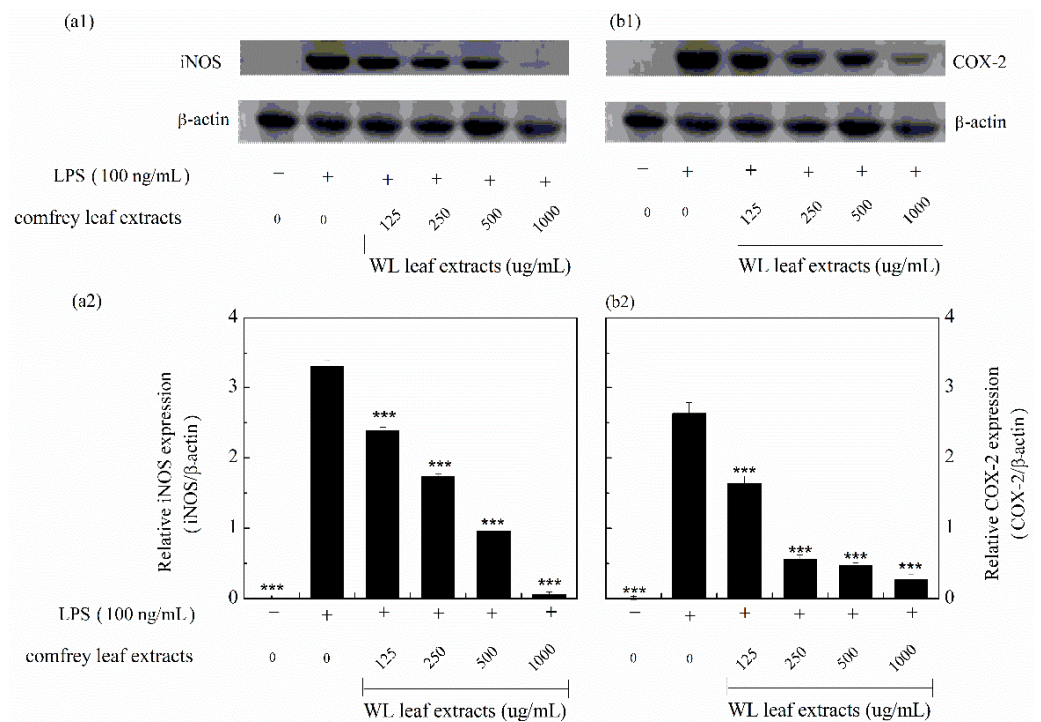


**Figure 7.** The iNOS (a1,a2) and COX-2 (b1,b2) productions of LPS-induced RAW264.7 macrophages treated with indicated concentrations of the WLE. Expression levels of iNOS and  $\beta$ -actin (a1) and COX-2 and  $\beta$ -actin (b1) were obtained by Western blotting. The relative iNOS (a2) and COX-2 (b2) expression levels were calculated. Treated with (+) or without (-) LPS and WLE, and the used concentrations of WLE were indicated. \*\*\* ( $p < 0.001$ ) denotes significant difference compared with the LPS-only treated group.

To decipher the signaling pathway(s) involved in the WLE suppressing LPS-induced inflammation, we evaluated the effects of the WLE on the MAPK signaling pathway, including ERK, JNK, and p38. Phosphate groups were added on ERK, JNK, and p38 when activated. Phosphorylated ERK (p-ERK), phosphorylated JNK (p-JNK), phosphorylated p38 (p-p38), total ERK (t-ERK), total JNK (t-JNK), and total p38 (t-p38) expression levels were obtained by Western blotting (Figure 9A). The percentage ratios of p-ERK to t-ERK (Figure 9B), p-JNK to t-JNK (Figure 9C), and p-p38 to t-p38 (Figure 9D) are shown. These results indicated that LPS treatment significantly increased all ratios of p-ERK to t-ERK, p-JNK to t-JNK, and p-p38 to t-p38. The WLE significantly reduced LPS-induced p-p38 to t-p38 ratios at 125–1000  $\mu\text{g}/\text{mL}$  concentrations. However, only higher concentrations ( $\geq 250$   $\mu\text{g}/\text{mL}$ ) of the WLE showed significant inhibitory effects on ratios of p-ERK to t-ERK and p-JNK to t-JNK. Thus, p38 is more reactive than ERK and JNK by the WLE. From the results of Figure 9, we identified that the WLE suppressed LPS-induced inflammation through the MAPK signaling pathway.

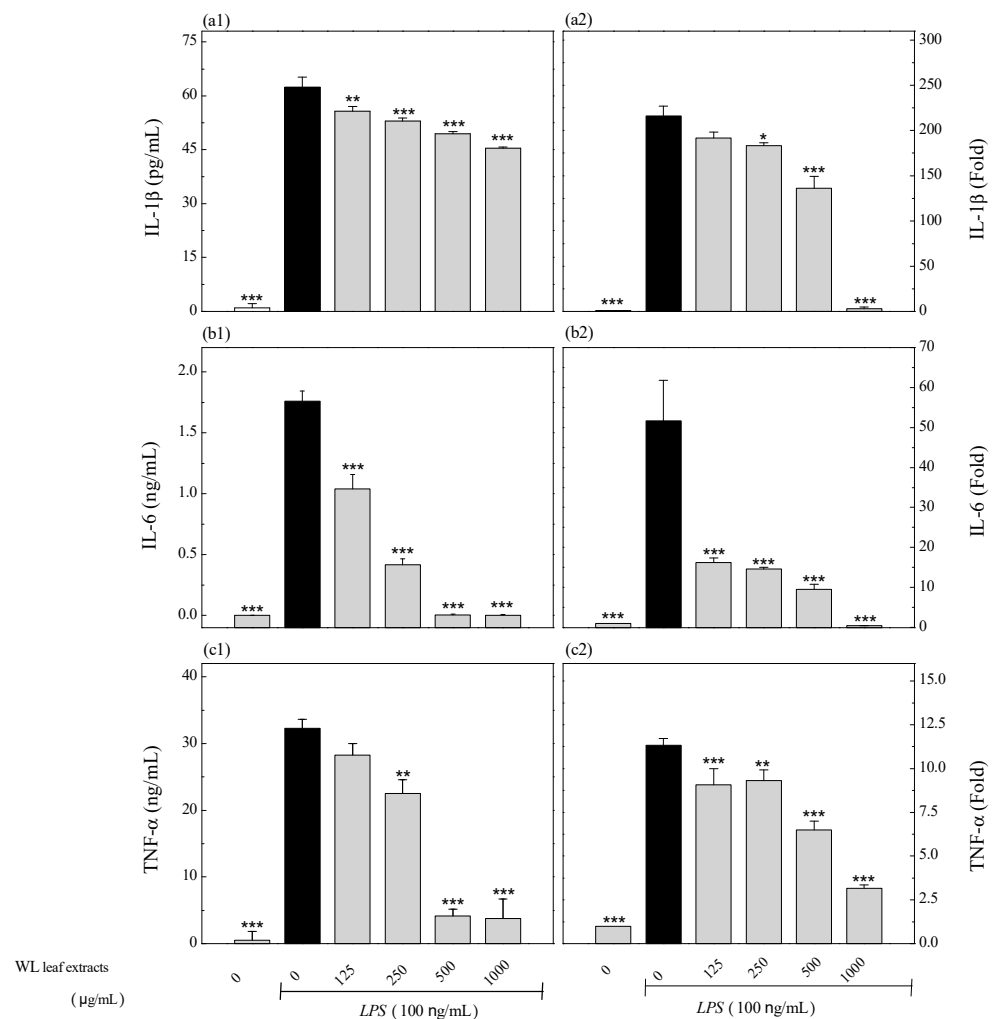


**Figure 8.** The relative expression levels of genes (a2,b2,c2) and proteins (a1,b1,c1) of LPS-induced RAW264.7 macrophages. RAW264.7 macrophages were treated with indicated concentrations of the WLE. The expression levels of analyzed genes in cells without LPS and the WLE were all designated 1.0-fold. Protein expression levels (a1,b1,c1) and relative folds of mRNA expression levels (a2,b2,c2) of IL-1β (a), IL-6 (b), and TNF-α (c) were calculated, respectively. Samples treated with LPS were underlined, and the used concentrations of the WLE were indicated. \* ( $p < 0.05$ ), \*\* ( $p < 0.01$ ), and \*\*\* ( $p < 0.001$ ) denote significant differences compared with the LPS-only treated group.

Furthermore, we determined whether the WLE regulated the NF-κB signaling pathway. The p65 is a crucial trans-activating domain of NF-κB. When activated, the phosphate group is added to p65, and then phosphorylated p65 (p-p65) is translocated from the cytoplasm into the nucleus. We assessed the expressions of p-p65 and total p65 (t-p65) by Western blotting (Figure 10A). Ratios in percentages of p-p65 to t-p65 were shown (Figure 10B). These results indicated that LPS treatments significantly increased the ratio of p-p65 to t-p65, and the WLE significantly reduced this elevation at concentrations of 500–1000 µg/mL. Furthermore, the results of immunofluorescence of p-p65 and DAPI indicated that LPS treatments significantly increased the nuclear level of p65 protein, and the WLE lessened the translocation of p65 protein. In brief, we also identified that the WLE suppressed LPS-induced inflammation through the NF-κB signaling pathway.

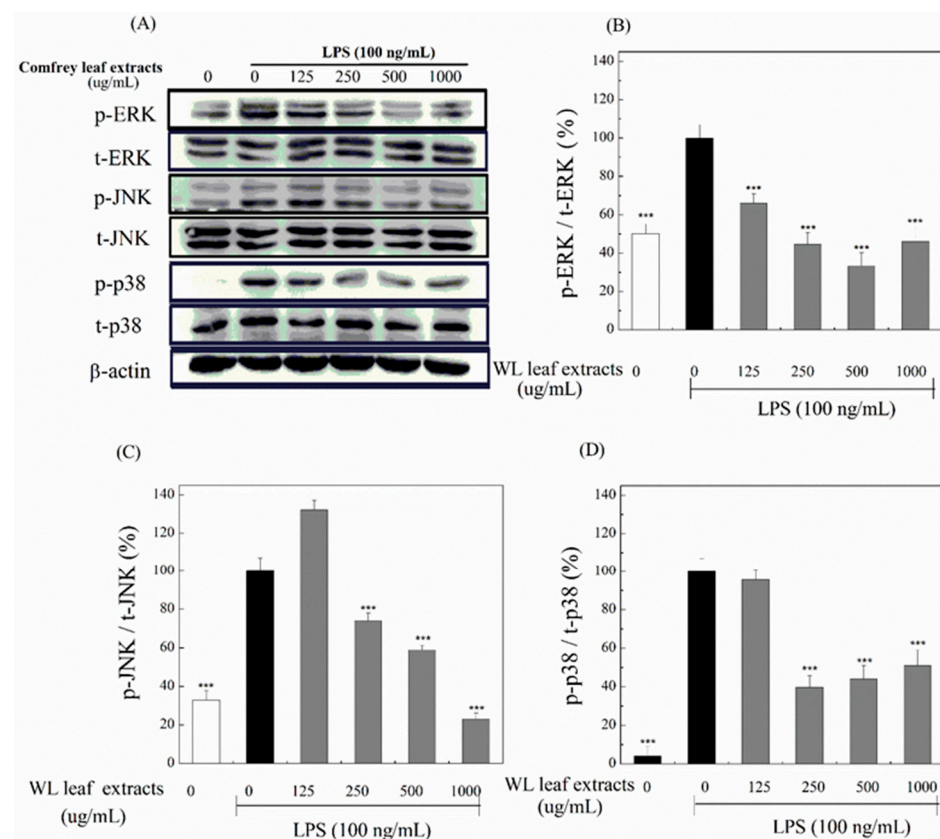


**Figure 9.** Attenuations of LPS-induced MAPK signaling by WLE. (A) Expression levels of phosphorylated ERK (p-ERK), phosphorylated JNK (p-JNK), phosphorylated p38 (p-p38), total ERK (t-ERK), total JNK (t-JNK), total p38 (t-p38), and  $\beta$ -actin were obtained by Western blotting. Percentage ratios of p-ERK to t-ERK (B), p-JNK to t-JNK (C), and p-p38 to t-p38 (D) were calculated, respectively. Samples treated with LPS were underlined, and the used concentrations of the WLE were indicated. \*\*\* ( $p < 0.001$ ) denotes significant difference compared with the LPS-only treated group.

MAPKs constitute an important cascade of inflammatory signaling from the cell surface to the nucleus. LPS interacts with Toll-like receptor 4, which then activates various MAPK pathways, including ERK, JNK, and p38, mediating the activation of pro-inflammatory transcription factors [53]. Activation of the NF- $\kappa$ B signaling pathway is closely related to activated MAPK, which can promote downstream transcription factors and increase the expression of inflammatory genes [54]. p38 has been identified as an upstream regulator of NF- $\kappa$ B, although the molecular mechanism of how p38 regulates NF- $\kappa$ B remains unclear [55]. Inhibition of p38 attenuates NF- $\kappa$ B activation; however, it does not affect nuclear NF- $\kappa$ B translocation and its DNA binding [56]. Therefore, blocking p38 can reduce the expression of NF- $\kappa$ B-mediated pro-inflammatory factor genes, including TNF- $\alpha$  and IL-1 $\beta$ , as well as inflammatory mediators COX-2 and iNOS [57,58]. In vitro and in vivo experiments have identified the phenolic compounds of comfrey as anti-inflammatory agents [59]. RA is a polyphenol thought to have anti-inflammatory and wound-healing properties of plants, including comfrey [60]. Thus, we conclude that RA in the WLE attenuates LPS-stimulated pro-inflammatory cytokines, including TNF- $\alpha$ , IL-1 $\beta$ , and IL-6, and inflammatory mediators, including iNOS and COX-2, through inhibition of both MAPK and NF- $\kappa$ B signaling pathways (Figure 11).

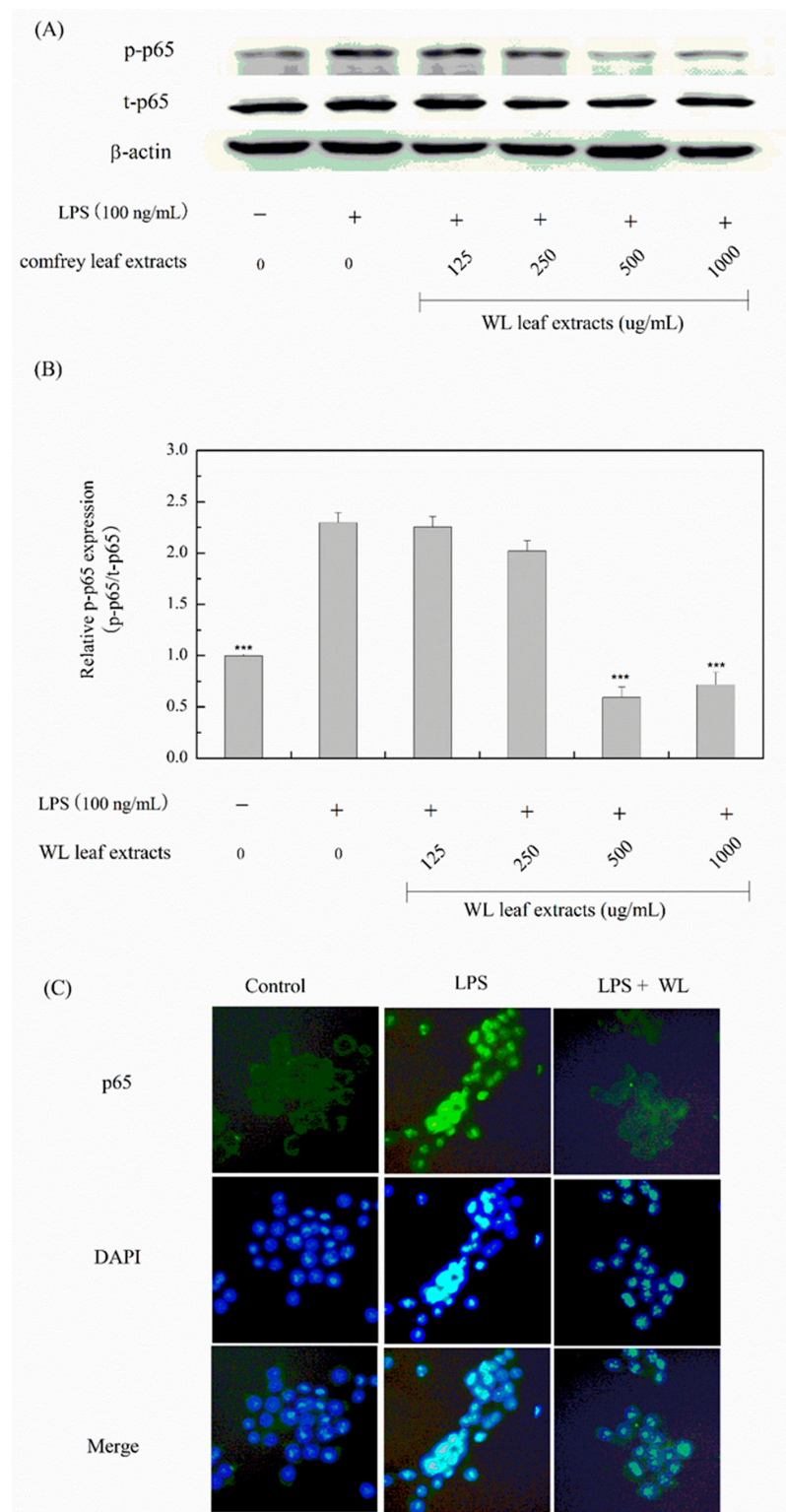


**Figure 10.** Attenuations of LPS-stimulated NF- $\kappa$ B signaling by the WLE. (A) Expression levels of phosphorylated p65 (p-p65), total p65 (t-p65), and  $\beta$ -actin were obtained by Western blotting. (B) Ratios in the fold of p-p65 to t-p65 were calculated. Treated with (+) or without (–) LPS and WLE were indicated. The used concentrations of WLE were indicated. \*\*\* ( $p < 0.001$ ) denotes significant difference compared with the LPS-only treated group. (C) Fluorescent images of p65 (**upper**), DAPI (**medium**), and merge (**lower**) in the control, LPS, and LPS + WLE groups, respectively.

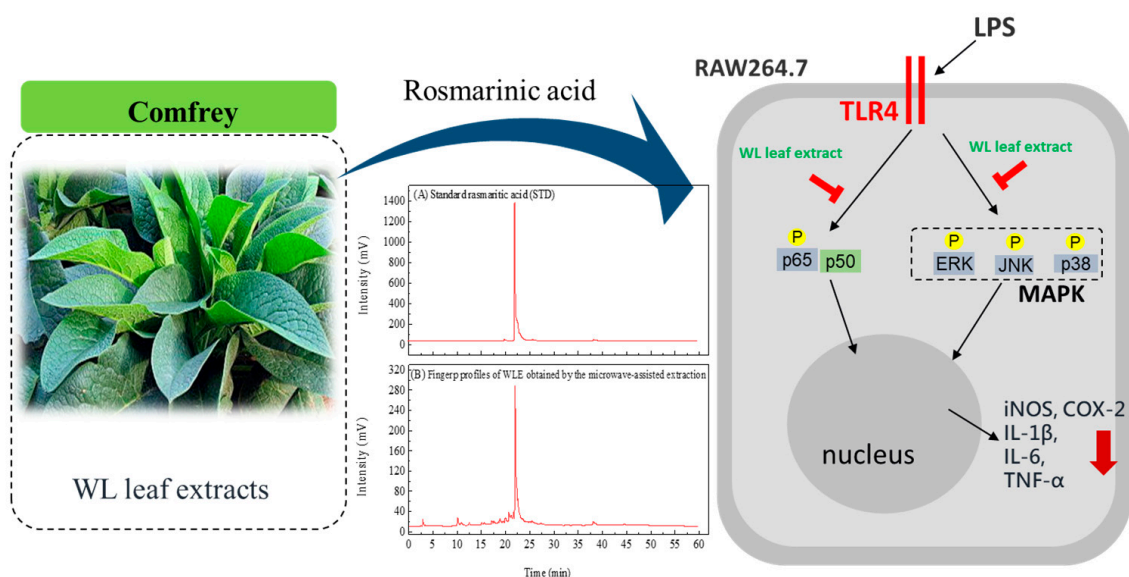


**Figure 11.** Schematic diagram of attenuating inflammation of LPS-induced RAW264.7 macrophages by WLE.

#### 4. Conclusions

A native comfrey plant was identified as *S. officinale* WL by molecular identification. Using MAE, the suitable extraction conditions of the WL leaves with high extraction yield and contents of total phenols and flavonoids were obtained with 750 W microwave power, 50 °C, 75% methanol, 1:10 solid-to-solvent ratio, and 15 min extraction duration. The WLE showed evident antioxidant capacity by assays of DPPH, ABTS, and SOD-like activities, reducing power, ferrous ion chelating activity, and FRAP. Furthermore, WLE showed the first reported DNA protective effect of comfrey extract by an in vitro study. Since high levels of phenolics and flavonoids are closely related to the antioxidant capacity of plant extracts, we hypothesized that phenolic and flavonoid compounds in the WLE are responsible for antioxidant capacity and DNA protection. The WLE also showed an apparent anti-inflammatory effect in LPS-stimulated RAW 264.7 macrophages. WLE was a potent inhibitor of LPS-induced IL-1 $\beta$ , IL-6, TNF- $\alpha$ , iNOS, and COX-2 productions in macrophages. The inhibitory mechanisms involved MAPK and NF- $\kappa$ B signaling pathways. RA is one of the polyphenols believed to be responsible for anti-inflammation and wound-healing properties. The WLE contained the highest RA concentration among all reported comfrey extracts by HPLC assay. We believe that the high RA concentration in WLE is responsible for the anti-inflammatory activity of WLE. Since our findings indicate that WLE has antioxidant, DNA protection, and anti-inflammation effects, our results demonstrate that the production of comfrey leaf extract by MAE may provide a safe and efficacious source of comfrey extract for pharmaceutical applications.

**Author Contributions:** Conceptualization, K.-H.L. and J.-Y.W.; methodology, M.-S.T. and J.-Y.W.; software, J.-Y.W.; validation, M.-S.T. and J.-Y.W.; formal analysis, J.-Y.W.; investigation, K.-H.L.; resources, K.-H.L. and J.-Y.W.; data curation, K.-H.L.; writing—original draft preparation, K.-H.L.; writing—review and editing, M.-S.T. and J.-Y.W.; visualization, J.-Y.W.; supervision, J.-Y.W.; project administration, K.-H.L.; funding acquisition, K.-H.L. All authors have read and agreed to the published version of the manuscript.

**Funding:** This research was funded by Paoenergy Technology Co., Ltd., grant number: SMI 2020123.

**Data Availability Statement:** The data presented in this study are available on request from the corresponding author. The data are not publicly available due to a potential patent application.

**Conflicts of Interest:** The authors declare no conflict of interest.

## References

1. DerMarderosian, A.H.; Beutler, J.A. *The Review of Natural Products: The Most Complete Source of Natural Product Information; Facts and Comparisons*: St. Louis, MO, USA, 2002.
2. Kadereit, J.W.; Bittrich, V. Eudicots: Aquifoliales, Boraginales, Bruniales, Dipsacales, Escalloniales, Garryales, Paracryphiales, Solanales (except Convolvulaceae), Icacinaceae, Metteniusaceae, Vahliaceae. In *Flowering Plants*, 1st ed.; Kadereit, J.W., Bittrich, V., Eds.; Springer International Publishing: Cham, Switzerland, 2016; pp. 41–102. [[CrossRef](#)]
3. Mahmoudzadeh, E.; Nazemiyeh, H.; Hamedeyazdan, S. Anti-inflammatory Properties of the Genus *Symphytum* L.: A Review. *Iran. J. Pharm. Res.* **2022**, *21*, e123949. [[CrossRef](#)] [[PubMed](#)]
4. Englert, K.; Mayer, J.G.; Staiger, C. *Symphytum officinale* L.—der Beinwell in der europäischen Pharmazie- und Medizingeschichte. *Z. Phytother.* **2005**, *26*, 158–168. [[CrossRef](#)]
5. Seigner, J.; Junker-Samek, M.; Plaza, A.; D’Urso, G.; Masullo, M.; Piacente, S.; Holper-Schichl, Y.M.; de Martin, R. A *Symphytum officinale* Root Extract Exerts Anti-inflammatory Properties by Affecting Two Distinct Steps of NF- $\kappa$ B Signaling. *Front. Pharmacol.* **2019**, *10*, 289. [[CrossRef](#)]
6. Sowa, I.; Paduch, R.; Strzemeski, M.; Zielińska, S.; Rydzik-Strzemska, E.; Sawicki, J.; Kocjan, R.; Polkowski, J.; Matkowski, A.; Latański, M.; et al. Proliferative and antioxidant activity of *Symphytum officinale* root extract. *Nat. Prod. Res.* **2018**, *32*, 605–609. [[CrossRef](#)] [[PubMed](#)]
7. Smith, D.B.; Jacobson, B.H. Effect of a blend of comfrey root extract (*Symphytum officinale* L.) and tannic acid creams in the treatment of osteoarthritis of the knee: Randomized, placebo-controlled, double-blind, multiclinical trials. *J. Chiropr. Med.* **2011**, *10*, 147–156. [[CrossRef](#)]
8. Neagu, E.; Roman, G.P.; Radu, G.L. Antioxidant capacity of some *Symphytum officinalis* extracts processed by ultrafiltration. *Rom. Biotechnol. Lett.* **2010**, *15*, 5505–5511.
9. Savić, V.L.; Savić, S.; Nikolić, V.; Nikolić, L.; Najman, S.J.; Lazarević, J.S.; Djordjević, A. The identification and quantification of bioactive compounds from the aqueous extract of comfrey root by UHPLC-DAD-HESI-MS method and its microbial activity. *Hem. Ind.* **2015**, *69*, 1–8. [[CrossRef](#)]
10. Salehi, B.; Sharopov, F.; Boyunegmez Tumer, T.; Ozleyen, A.; Rodríguez-Pérez, C.; Ezzat, S.M.; Azzini, E.; Hosseinabadi, T.; Butnariu, M.; Sarac, I.; et al. *Symphytum* Species: A Comprehensive Review on Chemical Composition, Food Applications and Phytopharmacology. *Molecules* **2019**, *24*, 2272. [[CrossRef](#)]
11. Trifan, A.; Opitz, S.E.W.; Josuran, R.; Grubelnik, A.; Esslinger, N.; Peter, S.; Bräm, S.; Meier, N.; Wolfram, E. Is comfrey root more than toxic pyrrolizidine alkaloids? Salvianolic acids among antioxidant polyphenols in comfrey (*Symphytum officinale* L.) roots. *Food Chem. Toxicol.* **2018**, *112*, 178–187. [[CrossRef](#)]
12. E.S.C.O. *Symphyti radix*, Comfrey root. In *E/S/C/O/P Monographs: The Scientific Foundation for Herbal Medicinal Products. Supplement 2009*, 2nd ed.; European Scientific Cooperative on Phytotherapy: Devon, UK, 2009; pp. 249–254.
13. Frost, R.; MacPherson, H.; O’Meara, S. A critical scoping review of external uses of comfrey (*Symphytum* spp.). *Complement. Ther. Med.* **2013**, *21*, 724–745. [[CrossRef](#)]
14. Frost, R.; O’Meara, S.; MacPherson, H. The external use of comfrey: A practitioner survey. *Complement. Ther. Clin. Pract.* **2014**, *20*, 347–355. [[CrossRef](#)]
15. Syarifah, A.N.; Suryadi, H.; Hayun, H.; Simamora, A.; Mun’im, A. Detoxification of comfrey (*Symphytum officinale* L.) extract using natural deep eutectic solvent (NADES) and evaluation of its anti-inflammatory, antioxidant, and hepatoprotective properties. *Front. Pharmacol.* **2023**, *14*, 1012716. [[CrossRef](#)]
16. Elez Garofulić, I.; Dragović-Uzelac, V.; Režek Jambrak, A.; Jukić, M. The effect of microwave assisted extraction on the isolation of anthocyanins and phenolic acids from sour cherry Marasca (*Prunus cerasus* var. Marasca). *J. Food Eng.* **2013**, *117*, 437–442. [[CrossRef](#)]
17. Tanongkankit, Y.; Sablani, S.S.; Chiewchan, N.; Devahastin, S. Microwave-assisted extraction of sulforaphane from white cabbages: Effects of extraction condition, solvent and sample pretreatment. *J. Food Eng.* **2013**, *117*, 151–157. [[CrossRef](#)]
18. Karavaev, V.A.; Solntsev, M.K.; Iurina, T.P.; Iurina, E.V.; Poliakova, I.B.; Kuznetsov, A.M. Antifungal activity of aqueous extracts from the leaf of cowparsnip and comfrey. *Izv. Akad. Nauk. Ser. Biol.* **2001**, *4*, 435–441.
19. Sumathi, S.; Kumar, S.S.; Bai, A.L.G. Evaluation of Phytochemical Constituents and Antibacterial Activities of *Symphytum officinale* L. *J. Pure Appl. Microbiol.* **2011**, *5*, 323–328.
20. Sumathi, S.; Kumar, S.; Bharathi, V.; Sathish, S. Antibacterial activity of the plant extract of *Symphytum officinale* L. against selected pathogenic bacteria. *Int. J. Res. Pharm. Sci.* **2011**, *2*, 92–94.
21. Araújo, L.U.; Reis, P.G.; Barbosa, L.C.; Saúde-Guimarães, D.A.; Grabe-Guimarães, A.; Mosqueira, V.C.; Carneiro, C.M.; Silva-Barcellos, N.M. In Vivo wound healing effects of *Symphytum officinale* L. leaves extract in different topical formulations. *Pharmazie* **2012**, *67*, 355–360. [[PubMed](#)]
22. Oberlies, N.H.; Kim, N.C.; Brine, D.R.; Collins, B.J.; Handy, R.W.; Sparacino, C.M.; Wani, M.C.; Wall, M.E. Analysis of herbal teas made from the leaves of comfrey (*Symphytum officinale*): Reduction of N-oxides results in order of magnitude increases in the measurable concentration of pyrrolizidine alkaloids. *Public Health Nutr.* **2004**, *7*, 919–924. [[CrossRef](#)]
23. Dresler, S.; Szymczak, G.; Wójcik, M. Comparison of some secondary metabolite content in the seventeen species of the Boraginaceae family. *Pharm. Biol.* **2017**, *55*, 691–695. [[CrossRef](#)]

24. Neagu, E.; Paun, G.; Albu, C.; Eremia, S.A.V.; Radu, G.L. Artemisia abrotanum and *Symphytum officinale* Polyphenolic Compounds-Rich Extracts with Potential Application in Diabetes Management. *Metabolites* **2023**, *13*, 354. [[CrossRef](#)] [[PubMed](#)]
25. Khanuja, S.P.S.; Shasany, A.K.; Darokar, M.P.; Kumar, S. Rapid Isolation of DNA from Dry and Fresh Samples of Plants Producing Large Amounts of Secondary Metabolites and Essential Oils. *Plant Mol. Biol. Rep.* **1999**, *17*, 74. [[CrossRef](#)]
26. Hacıoğlu, B.; Erik, S. Phylogeny of *Symphytum* L. (Boraginaceae) with special emphasis on Turkish species. *Afr. J. Biotechnol.* **2011**, *10*, 15483–15493. [[CrossRef](#)]
27. Kähkönen, M.P.; Hopia, A.I.; Vuorela, H.J.; Rauha, J.P.; Pihlaja, K.; Kujala, T.S.; Heinonen, M. Antioxidant activity of plant extracts containing phenolic compounds. *J. Agric. Food Chem.* **1999**, *47*, 3954–3962. [[CrossRef](#)] [[PubMed](#)]
28. Chang, C.C.; Yang, M.H.; Wen, H.M.; Chern, J.C. Estimation of Total Flavonoid Content in Propolis by Two Complementary Colorimetric Methods. *J. Food Drug Anal.* **2002**, *10*, 178–182. [[CrossRef](#)]
29. Lee, J.Y.; Cho, Y.R.; Park, J.H.; Ahn, E.K.; Jeong, W.; Shin, H.S.; Kim, M.S.; Yang, S.H.; Oh, J.S. Anti-melanogenic and anti-oxidant activities of ethanol extract of *Kummerowia striata*: *Kummerowia striata* regulate anti-melanogenic activity through down-regulation of TRP-1, TRP-2 and MITF expression. *Toxicol. Rep.* **2019**, *6*, 10–17. [[CrossRef](#)]
30. Re, R.; Pellegrini, N.; Proteggente, A.; Pannala, A.; Yang, M.; Rice-Evans, C. Antioxidant activity applying an improved ABTS radical cation decolorization assay. *Free Radic. Biol. Med.* **1999**, *26*, 1231–1237. [[CrossRef](#)]
31. Singh, N.; Rajini, P.S. Free radical scavenging activity of an aqueous extract of potato peel. *Food Chem.* **2004**, *85*, 611–616. [[CrossRef](#)]
32. Zhao, H.; Fan, W.; Dong, J.; Lu, J.; Chen, J.; Shan, L.; Lin, Y.; Kong, W. Evaluation of antioxidant activities and total phenolic contents of typical malting barley varieties. *Food Chem.* **2008**, *107*, 296–304. [[CrossRef](#)]
33. Kumar, V.; Rani, A.; Dixit, A.K.; Pratap, D.; Bhatnagar, D. A comparative assessment of total phenolic content, ferric reducing-antioxidative power, free radical-scavenging activity, vitamin C and isoflavones content in soybean with varying seed coat colour. *Food Res. Int.* **2010**, *43*, 323–328. [[CrossRef](#)]
34. Li, X. Improved pyrogallol autoxidation method: A reliable and cheap superoxide-scavenging assay suitable for all antioxidants. *J. Agric. Food Chem.* **2012**, *60*, 6418–6424. [[CrossRef](#)] [[PubMed](#)]
35. Jothy, S.L.; Chen, Y.; Kanwar, J.R.; Sasidharan, S. Evaluation of the Genotoxic Potential against H<sub>2</sub>O<sub>2</sub>-Radical-Mediated DNA Damage and Acute Oral Toxicity of Standardized Extract of *Polyalthia longifolia* Leaf. *Evid. Based Complement. Altern. Med.* **2013**, *2013*, 925380. [[CrossRef](#)] [[PubMed](#)]
36. Li, C.Y.; Cheng, S.E.; Wang, S.H.; Wu, J.Y.; Hsieh, C.W.; Tsou, H.K.; Tsai, M.S. The Anti-inflammatory Effects of the Bioactive Compounds Isolated from *Alpinia officinarum* Hance Mediated by the Suppression of NF-kappaB and MAPK Signaling. *Chin. J. Physiol.* **2021**, *64*, 32–42. [[CrossRef](#)]
37. Ruenroengklin, N.; Zhong, J.; Duan, X.; Yang, B.; Li, J.; Jiang, Y. Effects of various temperatures and pH values on the extraction yield of phenolics from litchi fruit pericarp tissue and the antioxidant activity of the extracted anthocyanins. *Int. J. Mol. Sci.* **2008**, *9*, 1333–1341. [[CrossRef](#)] [[PubMed](#)]
38. Rajaei, A.; Barzegar, M.; Hamidi Esfahani, Z.; Sahari, M.A. Optimization of Extraction Conditions of Phenolic Compounds from Pistachio (*Pistachia vera*) Green Hull through Response Surface Method. *J. Agric. Sci. Tech.* **2010**, *12*, 605–615.
39. Tsao, R.; Deng, Z. Separation procedures for naturally occurring antioxidant phytochemicals. *J. Chromatogr. B* **2004**, *812*, 85–99. [[CrossRef](#)]
40. Kurucu, S.; Kartal, M.; Choudary, M.I.; Topcu, G. Pyrrolizidine Alkaloids from *Symphytum sylvaticum* Boiss. subsp. sepulcrale. (Boiss. & Bal.) Greuter & Burdet var. sepulcrale and *Symphytum aintabicum* Hub.-Mor. & Wickens. *Turk. J. Chem.* **2002**, *26*, 195–199.
41. Drużyńska, B.; Stepniewska, A.; Wołosiak, R. The influence of time and type of solvent on efficiency of the extraction of polyphenols from green tea and antioxidant properties obtained extracts. *Acta Sci. Pol. Technol. Aliment.* **2007**, *6*, 27–36.
42. Khoddami, A.; Wilkes, M.A.; Roberts, T.H. Techniques for analysis of plant phenolic compounds. *Molecules* **2013**, *18*, 2328–2375. [[CrossRef](#)]
43. Üstün Alkan, F.; Anlas, C.; Ustuner, O.; Bakirel, T.; Sari, A. Antioxidant and proliferative effects of aqueous and ethanolic extracts of *Symphytum officinale* on 3T3 Swiss albino mouse fibroblast cell line. *Asian J. Plant Sci. Res.* **2014**, *4*, 62–68.
44. Goldstein, S.; Meyerstein, D.; Czapski, G. The Fenton reagents. *Free Radic. Biol. Med.* **1993**, *15*, 435–445. [[CrossRef](#)] [[PubMed](#)]
45. Burrows, C.J.; Muller, J.G. Oxidative Nucleobase Modifications Leading to Strand Scission. *Chem. Rev.* **1998**, *98*, 1109–1152. [[CrossRef](#)] [[PubMed](#)]
46. Spothem-Maurizot, M.; Franchet, J.; Sabbattier, R.; Charlier, M. DNA radiolysis by fast neutrons. II. Oxygen, thiols and ionic strength effects. *Int. J. Radiat. Biol.* **1991**, *59*, 1313–1324. [[CrossRef](#)]
47. Sestili, P.; Guidarelli, A.; Dachà, M.; Cantoni, O. Quercetin Prevents DNA Single Strand Breakage and Cytotoxicity Caused by tert-Butylhydroperoxide: Free Radical Scavenging Versus Iron Chelating Mechanism. *Free Radic. Biol. Med.* **1998**, *25*, 196–200. [[CrossRef](#)]
48. Ho, Y.S.; Wu, J.Y.; Chang, C.Y. A New Natural Antioxidant Biomaterial from *Cinnamomum osmophloeum* Kanehira Leaves Represses Melanogenesis and Protects against DNA Damage. *Antioxidants* **2019**, *8*, 474. [[CrossRef](#)] [[PubMed](#)]
49. Wang, W.-T.; Liao, S.-F.; Wu, Z.-L.; Chang, C.-W.; Wu, J.-Y. Simultaneous study of antioxidant activity, DNA protection and anti-inflammatory effect of *Vernonia amygdalina* leaves extracts. *PLoS ONE* **2020**, *15*, e0235717. [[CrossRef](#)]

50. Nastić, N.; Borrás-Linares, I.; Lozano-Sánchez, J.; Švarc-Gajić, J.; Segura-Carretero, A. Comparative Assessment of Phytochemical Profiles of Comfrey (*Symphytum officinale* L.) Root Extracts Obtained by Different Extraction Techniques. *Molecules* **2020**, *25*, 837. [[CrossRef](#)]
51. Surh, Y.J.; Chun, K.S.; Cha, H.H.; Han, S.S.; Keum, Y.S.; Park, K.K.; Lee, S.S. Molecular mechanisms underlying chemopreventive activities of anti-inflammatory phytochemicals: Down-regulation of COX-2 and iNOS through suppression of NF-kappa B activation. *Mutat. Res.* **2001**, *480–481*, 243–268. [[CrossRef](#)]
52. Feldmann, M. Cytokine networks: Do we understand them well enough to facilitate clinical benefits? *Eur. Cytokine Netw.* **1991**, *2*, 5–9.
53. Guha, M.; Mackman, N. LPS induction of gene expression in human monocytes. *Cell Signal.* **2001**, *13*, 85–94. [[CrossRef](#)]
54. Saklatvala, J. Inflammatory signaling in cartilage: MAPK and NF-kappaB pathways in chondrocytes and the use of inhibitors for research into pathogenesis and therapy of osteoarthritis. *Curr. Drug Targets* **2007**, *8*, 305–313. [[CrossRef](#)] [[PubMed](#)]
55. Hehner, S.P.; Hofmann, T.G.; Ratter, F.; Dumont, A.; Dröge, W.; Schmitz, M.L. Tumor necrosis factor-alpha-induced cell killing and activation of transcription factor NF-kappaB are uncoupled in L929 cells. *J. Biol. Chem.* **1998**, *273*, 18117–18121. [[CrossRef](#)] [[PubMed](#)]
56. Saha, R.N.; Jana, M.; Pahan, K. MAPK p38 regulates transcriptional activity of NF-kappaB in primary human astrocytes via acetylation of p65. *J. Immunol.* **2007**, *179*, 7101–7109. [[CrossRef](#)] [[PubMed](#)]
57. Guo, W.; Sun, J.; Jiang, L.; Duan, L.; Huo, M.; Chen, N.; Zhong, W.; Wassy, L.; Yang, Z.; Feng, H. Imperatorin attenuates LPS-induced inflammation by suppressing NF-κB and MAPKs activation in RAW 264.7 macrophages. *Inflammation* **2012**, *35*, 1764–1772. [[CrossRef](#)] [[PubMed](#)]
58. Reddy, D.B.; Reddanna, P. Chebulagic acid (CA) attenuates LPS-induced inflammation by suppressing NF-κB and MAPK activation in RAW 264.7 macrophages. *Biochem. Biophys. Res. Commun.* **2009**, *381*, 112–117. [[CrossRef](#)] [[PubMed](#)]
59. Chen, L.; Teng, H.; Xie, Z.; Cao, H.; Cheang, W.S.; Skalicka-Woniak, K.; Georgiev, M.I.; Xiao, J. Modifications of dietary flavonoids towards improved bioactivity: An update on structure-activity relationship. *Crit. Rev. Food. Sci. Nutr.* **2018**, *58*, 513–527. [[CrossRef](#)]
60. Kučera, M.; Barna, M.; Horáček, O.; Kováriková, J.; Kučera, A. Efficacy and safety of topically applied *Symphytum* herb extract cream in the treatment of ankle distortion: Results of a randomized controlled clinical double-blind study. *Wien. Med. Wochenschr.* **2004**, *154*, 498–507. [[CrossRef](#)]

**Disclaimer/Publisher’s Note:** The statements, opinions and data contained in all publications are solely those of the individual author(s) and contributor(s) and not of MDPI and/or the editor(s). MDPI and/or the editor(s) disclaim responsibility for any injury to people or property resulting from any ideas, methods, instructions or products referred to in the content.